antigen.[19,20] Antibody units were calculated from the OD_{450} results, based on a standard curve obtained from serial concentrations of pooled plasma with a high titer of IgG anti-GPIIb/IIIa antibodies at dilutions ranging from 1:50 to 1:6400. One unit of anti-GPIIb/IIIa antibody was defined as the amount present in the pooled plasma diluted 1:3200. All samples were examined in duplicate, and the results were calculated as the mean of two values. An abnormal value for platelet-associated antibody was defined as ≥ 3.3 units and an abnormal value for plasma anti-GPIIb-IIIa antibody was defined as ≥ 5.0 units, based on 5 standard deviations above the mean obtained from 40 healthy persons.

Evaluation of platelet turnover

Reticulated platelets were detected by staining platelets with thiazole orange (Retic-COUNT, Becton Dickinson, San Jose, Calif) followed by the flow cytometric analysis described previously.[21,22] The fluorescence histogram was analyzed using a linear gate set to capture 1% of the reticulated platelet counts. This standard gate was used to analyze data from all samples and measure the percentage of thiazole orange-positive platelets in this gate. When a single such marker was used to analyze a series of 40 healthy control samples to determine the variability of the technique, the average percentage of reticulated platelets was 0.85% ± 0.23% (range, 0.2% to 1.5%). An abnormal value for the percentage of reticulated platelets was defined as greater than the mean plus 5 standard deviations (2.0%) in our assay system. Possible day-to-day variability was assessed in 2 healthy control subjects; the inter-assay coefficient of variation was 9.6%, and the intra-assay coefficient of variation was 5.4%. The plasma thrombopoietin level was measured using a commercially available enzyme-linked immunosorbent assay kit (Quantikine; R&D Systems, Minneapolis, Minn) according to the manufacturer's protocol. The mean plasma thrombopoietin level in 30 healthy persons was 83.9 ± 11.7 pg/mL (range, 50 to 126 pg/mL). A thrombopoietin level of ≥ 142 pg/mL was defined as abnormal based on a normal mean plus 5 standard deviations.

Statistical analysis

Confidence intervals were calculated for each sensitivity, specificity, positive predictive value, and negative predictive value. Comparisons between 2 patient groups were tested for statistical significance using the nonparametric Mann-Whitney test or the chi-squared test, as appropriate.

Results

Clinical diagnosis of patients with thrombocytopenia

For the 62 patients, the clinical diagnosis was ITP in 46 patients (74%), myelodysplastic syndrome in 8 (13%), aplastic anemia in 2 (3%), and amegakaryocytic thrombocytopenia in 1 (2%). Five patients (8%) did not have a definitive final diagnosis at the last observation (observation period ranged from 11 to 23 months), because they continued to have reduced megakaryocytes in the bone marrow, alone or in combination with other lineages, without morphologic evidence for dysplasia. These patients were tentatively diagnosed as having reduced platelet production, with or without other cytopenias, and without dysplasia or evidence for platelet destruction. Among the 46 patients with a diagnosis of ITP, 32 received corticosteroids and showed a subsequent partial or complete response. Three patients who were refractory to corticosteroid therapy underwent splenectomy, which successfully increased the platelet count. All 6 patients who were treated with intravenous immunoglobulin experienced an increase in platelet count. Five patients with ITP were treated for *Helicobacter pylori*, and 3 showed a significant increase in platelet count after the successful eradication.

Clinical and laboratory findings in ITP versus non-ITP

The initial findings for evaluation of anti-GPIIb/IIIa antibody responses and platelet turnover were compared according to final clinical diagnosis (Figure). High levels of anti-GPIIb/IIIa antibody-producing B cell frequency, platelet-associated anti-GPIIb/IIIa antibodies, and the percentage of reticulated platelets were detected almost exclusively in patients who later received a final diagnosis of ITP. The plasma thrombopoietin level was normal or slightly increased in patients with ITP, but more than half the patients with myelodysplastic syndrome, aplastic anemia, amegakaryocytic thrombocytopenia, or reduced platelet production, with or without other cytopenias, without dysplasia or evidence for platelet destruction, had an extremely high plasma thrombopoietin level. An increased level of plasma anti-GPIIb/IIIa antibodies was found in only a small number of patients, irrespective of the final diagnosis.

The 46 patients with a final diagnosis of ITP tended to be younger than the 16 patients with other diagnoses (Table 1). Six laboratory findings, including the presence or absence of anemia, the leukocyte count, the frequency of anti-GPIIb/IIIa antibody-producing B cells, the platelet-associated anti-GPIIb/IIIa antibody level, the percentage of reticulated platelets, and the plasma thrombopoietin level, were different at presentation in patients later diagnosed as having ITP than in other patients. The initial platelet count was marginally lower in ITP compared with other diagnoses. The sensitivity, specificity, positive predictive value, and negative predictive value for each of these laboratory findings (Table 2) showed that no single test was sufficient to diagnose ITP in patients with thrombocytopenia. The combination of 3 simple and inexpensive tests (anemia, leukocyte count, and reticulated platelets) also had a low sensitivity and negative predictive value, but the addition of any one of

the substantially more costly tests improved sensitivity and negative predictive value (Table 3). When the presence of 3 or more of the 6 initial ITP-associated laboratory findings was regarded as possible ITP, a positive result was detected in 44 of 46 patients ultimately diagnosed as ITP (96%) but in only 1 (6%) of 16 patients without ITP, indicating a sensitivity of 96%, specificity of 94%, positive predictive value of 98%, and negative predictive value of 88%.

Discussion

This prospective study demonstrates that 6 laboratory tests (erythrocyte count, leukocyte count, anti-GPIIb/IIIa antibody-producing B cells, platelet-associated anti-GPIIb/IIIa antibodies, reticulated platelets, and plasma thrombopoietin level) performed at the first visit are useful to predict a future diagnosis of ITP. These laboratory findings associated with the diagnosis of ITP are categorized into 3 groups that individually reflect different aspects of the disease: a lack of abnormality in myeloid and erythroid lineages, the presence of autoantibody response to platelet-specific GPIIb/IIIa, and preserved platelet production. Three simple and inexpensive tests plus at least 1 of the other more costly ITP-associated laboratory tests measured together at first visit were a relatively sensitive and specific way to discriminate between the future diagnosis of ITP as compared with other conditions. However, it was difficult to determine which combination was most reasonable, probably because the number of patients examined in this study was relatively small. Further multicenter studies involving larger patient cohorts are necessary to make a decision regarding the least expensive and more efficient combination of laboratory tests to detect ITP.

To evaluate the autoimmune nature of the disease, the autoantibody response to GPIIb/IIIa, a major target of antiplatelet autoantibodies, was examined using 2 different methods that have complementary advantages and disadvantages. The enzyme-linked immunospot assay is very sensitive, but this assay system detects B cells that produce antibodies reacting with immobilized GPIIb/IIIa irrespective of their capacity to bind platelet surfaces. This assay would therefore give a false-positive result in patients who have antibodies that react with GPIIb/IIIa but fail to bind platelet surfaces, ie, antibodies that recognize a cytoplasmic domain of GPIIIa.[23] This result may have occurred in 1 of the patients with myelodysplastic syndrome, who showed highly positive results with anti-GPIIb/IIIa antibody-producing B cells and plasma anti-GPIIb/IIIa antibodies but who did not have platelet-associated anti-GPIIb/IIIa antibodies. Conversely, immunologic assays for platelet-associated anti-GPIIb/IIIa antibodies specifically detect antibodies capable of binding platelet surfaces, although the sensitivity is somewhat low.[7,9,10,24] The plasma anti-GPIIb/IIIa antibody level was not useful in the diagnosis of ITP, as reported previously,[20,24] because the majority of pathogenic anti-GPIIb/IIIa antibodies capable of binding platelets are present on platelet surfaces, rather than in the circulation. An increase in sensitivity might be achieved by simultaneously measuring the autoantibody response to other platelet-specific GP, such as GPIb/IX.[8]

Reticulated platelets are young platelets that have been recently released into the circulation and contain elevated levels of nucleic acid components.[25] The proportion of reticulated platelets among circulating platelets reflects platelet turnover.[21,22] Thrombopoietin is a principal regulator of megakaryo-thrombopoiesis, and its circulating level is inversely correlated with the absolute number of bone-marrow megakaryocytes and platelets.[26] These parameters are rapid, noninvasive tests that provide information about activity of the megakaryocytes in the bone marrow and platelet life span. Our prospective study showed that these convenient tests are useful for discriminating between ITP and hypoplastic thrombocytopenia, consistent with previous reports.[12-15]

In summary, initial laboratory findings that predicted future diagnosis of ITP identified in this study could potentially be included in future diagnostic criteria for adult ITP. Because the various combinations of diagnostic tests were retrospectively classified in this study, prospective evaluation of the same diagnostic criteria on another, independent set of patients is necessary.

References

1. Handin RI. Bleeding and thrombosis. In: Fauci AS, Braunwald E, Isselbacher KJ, et al., eds. *Harrison's Principles of Internal Medicine.* 14th ed. New York, New York: McGraw-Hill; 1998:339–345.
2. George JN, Rizvi MA. Thrombocytopenia. In: Beutler E, Lichtman MA, Coller BS, et al., *Williams* Hematology. 6th ed. New York, New York: McGraw-Hill; 2000:1495–1539.
3. Cines DB, Blanchette VS. Immune thrombocytopenic purpura. *N Engl J Med.* 2002;346:995–1008.
4. George JN, Woolf SH, Raskob GE, et al. Idiopathic thrombocytopenic purpura: A practice guideline developed by explicit methods for the American Society of Hematology. *Blood.* 1996;88:3–40.
5. British Committee for Standards in Haematology General Haematology Task Force. Guidelines for the investigation and management of idiopathic thrombocytopenic purpura in adults, children and in pregnancy. *Br J Haematol.* 2003;120:574–596.
6. Chong BH, Keng TB. Advances in the diagnosis of idiopathic thrombocytopenic purpura. *Semin Hematol.* 2000;37:249–260.
7. McMillan R, Wang L, Tani P. Prospective evaluation of the immunobead assay for the diagnosis of adult chronic immune thrombocytopenic purpura (ITP). *J Thromb Haemost.* 2003;1:485–491.
8. McMillan R. Autoantibodies and autoantigens in chronic immune thrombocytopenic purpura. *Semin Hematol.* 2000;37:239–248.
9. Brighton TA, Evans S, Castaldi PA, et al. Prospective evaluation of the clinical usefulness of an antigen-specific assay (MAIPA) in idiopathic thrombocytopenic purpura and other immune thrombocytopenias. *Blood.* 1996;88:194–201.
10. Warner MN, Moore JC, Warkentin TE, et al. A prospective study of protein-specific assays used to investigate idiopathic thrombocytopenic purpura. *Br J Haematol.* 1999;104:442–447.
11. Kuwana M, Okazaki Y, Kaburaki J, Ikeda Y. Detection of circulating B cells secreting platelet-specific autoantibody is a sensitive and spe-

cific test for the diagnosis of autoimmune thrombocytopenia. *Am J Med.* 2003;114:322–325.
12. Rinder HM, Munz UJ, Ault KA, et al. Reticulated platelets in the evaluation of thrombopoietic disorders. *Arch Pathol Lab Med.* 1993; 117:606–610.
13. Richards EM, Baglin TP. Quantitation of reticulated platelets: methodology and clinical application. *Br J Haematol.* 1995;9:445–451.
14. Koike Y, Yoneyama A, Shirai J, et al. Evaluation of thrombopoiesis in thrombocytopenic disorders by simultaneous measurement of reticulated platelets of whole blood and serum thrombopoietin concentrations. *Thromb Haemost.* 1998;79:1106–1110.
15. Kurata Y, Hayashi S, Kiyoi T, et al. Diagnostic value of tests for reticulated platelets, plasma glycocalicin, and thrombopoietin levels for discriminating between hyperdestructive and hypoplastic thrombocytopenia. *Am J Clin Pathol.* 2001;115:656–664.
16. Barrett J, Sauntharajah Y, Molldrem J. Myelodysplastic syndrome and aplastic anemia: distinct entities or diseases linked by a common pathophysiology? *Semin Hematol.* 2000;37:15–29.
17. Guinan EC. Clinical aspects of aplastic anemia. *Hematol Oncol Clin North Am.* 1997;11:1025–1044.
18. Manoharan A, Williams NT, Sparrow R. Acquired amegakaryocytic thrombocytopenia: report of a case and review of literature. *Q J Med.* 1989;70:243–252.
19. Kuwana M, Okazaki Y, Kaburaki J, et al. Spleen is a primary site for activation of glycoprotein IIb-IIIa-reactive T and B cells in patients with immune thrombocytopenic purpura. *J Immunol.* 2002;168: 3675–3682.
20. Hürlmann-Forster M, Steiner B, von Felten A. Quantitation of platelet-specific autoantibodies in platelet eluates of ITP patients measured by a novel ELISA using purified glycoprotein complexes GPIIb/IIIa and GPIb/IX as antigens. *Br J Haematol.* 1997;98:328–335.
21. Ault KA, Rinder HM, Mitchell J, et al. The significance of platelets with increased RNA content (reticulated platelets). A measure of the rate of thrombopoiesis. *Am J Clin Pathol.* 1992;98:637–646.
22. Saxon BR, Blanchette VS, Butchart S, et al. Reticulated platelet counts in the diagnosis of acute immune thrombocytopenic purpura. *J Pediatr Hematol Oncol.* 1998;20:44–48.
23. Fujisawa K, O'Toole TE, Tani P, et al. Autoantibodies to the presumptive cytoplasmic domain of platelet glycoprotein IIIa in patients with chronic immune thrombocytopenic purpura. *Blood.* 1991;77:2207–2213.
24. Berchtold P, Müller D, Beardsley D, et al. International study to compare antigen-specific methods used for the measurement of antiplatelet autoantibodies. *Br J Haematol.* 1997;96:477–483.
25. Ingram M, Coopersmith A. Reticulated platelets following acute blood loss. *Br J Haematol.* 1969;17:225–229.
26. Kaushansky K. Thrombopoietin: a tool for understanding thrombopoiesis. *J Thromb Haemost.* 2003;1:1587–1592.

Donor Fibroblast Chimerism in the Pathogenic Fibrotic Lesion of Human Chronic Graft-Versus-Host Disease

Yoko Ogawa,[1,2] *Hiroaki Kodama,*[3] *Kaori Kameyama,*[4] *Kazuto Yamazaki,*[4] *Hidekata Yasuoka,*[3] *Shinichiro Okamoto,*[3] *Hidetoshi Inoko,*[5] *Yutaka Kawakami,*[1] *and Masataka Kuwana*[1]

Purpose. Tissue atrophy and excessive fibrosis are prominent histologic features of chronic graft-versus-host disease (GVHD) after allogeneic hematopoietic stem cell transplantation, but the underlying mechanism remains unknown. The current study was undertaken to investigate whether the increase in fibroblasts at the site of pathogenic fibrosis originated from transplanted donor cells in patients with chronic GVHD.

Methods. Lacrimal gland biopsy specimens were obtained from nine patients with chronic GVHD. The male-specific sequences detected by fluorescein in situ hybridization (FISH) and in situ hybridization (ISH) were used as markers for the donor cells in seven female patients who had received a transplant from male donors. Primary fibroblast cultures were generated from lacrimal gland biopsy specimens and examined for mismatched genetic markers between recipients and donors.

Results. In lacrimal gland specimens obtained from seven female patients who received a sex-mismatched transplant, 13.4% to 26.7% of $CD34^+$ fibroblasts that accumulated in the fibrotic lesion were donor derived, as determined by FISH for the Y-chromosome. The male-specific mRNA was also detected in the lacrimal gland fibroblasts by ISH. Primary lacrimal gland fibroblast cultures were generated from four patients with chronic GVHD and further examined for mismatched genetic markers between recipients and donors. As a result, the presence of donor origin of the fibroblasts was demonstrated by detecting the Y-chromosome sequence and donor-specific microsatellite genetic markers.

Conclusions. These findings together indicate the chimeric status of accumulated $CD34^+$ fibroblasts in the lacrimal gland of patients with chronic GVHD. Fibroblasts originating from circulating donor-derived precursors may participate in the excessive fibrosis in these patients. (*Invest Ophthalmol Vis Sci.* 2005;46:4519-4527) DOI:10.1167/iovs.05-0227

Graft-versus-host disease (GVHD) is a major cause of morbidity and mortality in patients undergoing allogeneic hematopoietic stem cell transplantation (HSCT) for hematologic malignancies.[1] Acute GVHD is a distinctive syndrome of dermatitis, hepatitis, and enteritis that occurs soon after HSCT.[1] The pathogenic process of acute GVHD is explained as an alloimmune response of donor lymphocytes to recipient cells, followed by dysregulated cytokine production and the recruitment of additional effector cells.[2] In contrast, chronic GVHD is a more pleiotropic syndrome that develops several months after transplantation and frequently affects the skin, lung, liver, gastrointestinal tract, mouth, and eye.[1] The main histologic feature of chronic GVHD is widespread tissue atrophy and fibrosis with lymphocytic infiltration,[3] but less is understood about the pathophysiology of the condition.[1,4]

Dry eye has been recognized as a major complication in patients in whom chronic GVHD develops after allogeneic HSCT.[5-7] In most cases, severe dry eye progresses rapidly after the onset of symptoms and sometimes leads to blindness. Because of the increasing number of long-lived survivors who have received allogeneic HSCT, dry eye has a significant impact on these patients' quality of life. However, the pathogenic process of dry eye associated with chronic GVHD remains largely unknown.

We have been examining the pathogenesis of chronic GVHD by focusing on lacrimal gland involvement, one of the most frequent complications in the disease.[7-9] The main histologic findings in the affected lacrimal gland are marked fibrosis of the interstitium and a prominent increase in the number of $CD34^+$ fibroblasts accompanied by mild lymphocytic infiltration. Clinically, the severity of the dry eye correlates with the degree of fibrotic changes, rather than of lymphocytic infiltration, indicating that excessive extracellular matrix accumulation primarily contributes to the exocrine dysfunction. The $CD34^+$ fibroblasts at the interstitium also play a role in inflammation, in which the fibroblasts attach to lymphocytes and express human leukocyte antigen class II and costimulatory molecules. These findings together indicate that $CD34^+$ fibroblasts play an important role in the pathogenesis of lacrimal gland chronic GVHD.

Recently, several studies have reported the presence of donor-derived nonhematopoietic cells in various organs of HSCT recipients. These include neurons of the central nervous system,[10] gastric and intestinal epithelium,[11,12] subepithelial myofibroblasts of the intestine,[13] hepatocytes, keratinocytes,[12] and buccal epithelial cells.[14] These donor-derived cells are thought to play a role in regenerating the damaged tissues, but their proportion is very small. Several in vivo studies involving animal models, however, indicate that bone marrow–derived fibroblasts contribute to wound repair[15] and even to the development of pathogenic fibrosis.[16] These observations led us to hypothesize that a subset of the fibroblasts increased at the chronic GVHD lesion originated from transplanted donor cells. To test this hypothesis, we evaluated the origin of the $CD34^+$ fibroblasts that accumulate in the chronic GVHD lacrimal gland by detecting mismatched genetic markers in tissue specimens as well as in primary cultures of fibroblasts.

From the [1]Institute for Advanced Medical Research and the Departments of [2]Ophthalmology, [3]Internal Medicine, and [4]Diagnostic Pathology, Keio University School of Medicine, Tokyo, Japan; and the [5]Department of Molecular Life Science, Tokai University School of Medicine, Kanagawa, Japan.

Supported by grants from the Japanese Ministry of Education, Science, Sports and Culture.

Submitted for publication February 21, 2005; revised July 6, 2005; accepted September 29, 2005.

Disclosure: **Y. Ogawa**, None; **H. Kodama**, None; **K. Kameyama**, None; **K. Yamazaki**, None; **H. Yasuoka**, None; **S. Okamoto**, None; **H. Inoko**, None; **Y. Kawakami**, None; **M. Kuwana**, None

The publication costs of this article were defrayed in part by page charge payment. This article must therefore be marked "*advertisement*" in accordance with 18 U.S.C. §1734 solely to indicate this fact.

Corresponding author: Masataka Kuwana, Institute for Advanced Medical Research, Keio University School of Medicine, 35 Shinanomachi, Shinjuku, Tokyo 160-8582, Japan; kuwanam@sc.itc.keio.ac.jp.

Materials and Methods

Study Subjects

We studied nine allogeneic HSCT recipients who had clinically significant dry eye[17] and who had a diagnosis of chronic GVHD.[18] Lacrimal gland biopsy specimens that had been obtained for diagnostic purposes were available in all patients. Seven patients were women who had received sex-mismatched HSCTs from male donors (male-to-female recipients) with full donor lymphohematologic engraftment. A male patient who had received an HSCT from a male donor (male-to-male recipient) and a female patient who had received an HSCT from a female donor (female-to-female recipient) principally served as control subjects. All recipients underwent a myeloablative regimen consisting of total body irradiation in combination with cytosine arabinoside or cyclophosphamide, or a combination of fludarabine and melphalan. Peripheral blood mononuclear cells, bone marrow cells, and Epstein-Barr virus (EBV)-transformed B-cell line (BCL) obtained from recipients before and after HSCT as well as donor-derived peripheral blood mononuclear cells and bone marrow cells were used as a source of genomic DNA. Dry eye was diagnosed according to the diagnostic criteria proposed by Lemp,[17] with some modifications: Any sign of tear film instability (tear break-up time [BUT] $\leq$5 seconds, Schirmer test $\leq$5 mm, or cotton thread test $\leq$10 mm), and any abnormality of the ocular surface (rose-bengal score $\geq$3, fluorescein score $\geq$1), and/or symptoms of ocular irritation. Severe dry eye was defined as reduced reflex tearing (Schirmer test with nasal stimulation $\leq$10 mm) and ocular surface abnormality (rose-bengal score $\geq$3 and/or fluorescein score $\geq$1).[7,19] In some experiments, the lacrimal gland tissue obtained from a female patient with Sjögren's syndrome was used as a control. Written informed consent was obtained in advance from all patients in accordance with the principles expressed in the Declaration of Helsinki. This study was approved by the Keio University Institutional Review Boards.

Lacrimal Gland Specimens

Lacrimal gland tissues obtained by biopsy were divided into pieces and subjected to histologic analysis and primary culturing of fibroblasts. For culture, a portion of the tissue was placed on fibronectin-coated plastic plates and cultured in Dulbecco's modified Eagle's medium (Sigma-Aldrich, St. Louis, MO) with 10% heat-inactivated fetal bovine serum (JRH Biosciences, Lenexa, KS), 50 U/mL penicillin, and 50 μg/mL streptomycin without any exogenous growth factor. Proliferating adherent cells were passaged and expanded, and the cells at the third to fifth passage were used as cultured fibroblasts. In some experiments, a primary culture of fibroblasts generated from the skin biopsy of a female volunteer was used as a control.

Immunohistochemistry

Formalin-fixed, paraffin-embedded specimens were subjected to hematoxylin and eosin staining or CD34 immunostaining. For diaminobenzidine staining, anti-CD34 monoclonal antibody (mAb; NU-4A1; Nichirei, Tokyo, Japan) and peroxidase-conjugated secondary Ab (En Vision+; Dako, Glostrup, Denmark) were used in combination with nuclear staining with hematoxylin. For fluorescent staining, a fluorescein isocyanate (FITC)-conjugated anti-CD34 mAb (43A1; Calbiochem, San Diego, CA) was used in combination with TO-PRO-3 nuclear staining (Molecular Probes, Eugene, OR) for 1 hour at room temperature. Double staining of frozen sections was also performed with FITC-conjugated anti-CD34 mAb in combination with mouse anti-CD45 (PD7/26; Dako) or anti-CD90 mAb (AS02; Dianova, Hamburg, Germany) followed by inoculation with Alexa 568-conjugated rabbit anti-mouse IgG antibody (Molecular Probes) for 1 hour at room temperature. Isotype-matched mAbs to irrelevant antigen were used as controls in all tissue staining. The sections were mounted and examined with a confocal microscope (LSM5 Pascal; Carl-Zeiss Meditec, Göttingen, Germany).

Cultured fibroblasts were fixed with 4% paraformaldehyde for 10 minutes at room temperature and incubated with FITC-conjugated anti-CD34 mAb for 1 hour at room temperature. The cells were also incubated with mouse mAb to CD90, vimentin (V9; Dako), collagen type I (I-8H5; Daiichi Fine Chemical, Takaoka City, Japan), CD45, or pancytokeratin (mAb cocktail; Triton Bioscience, Alameda, CA), or rabbit polyclonal Ab to factor VIII (Dako) in combination with a tetramethylrhodamine isothiocyanate isomer R (TRITC)-conjugated anti-mouse or anti-rabbit IgG antibodies (Dako) for 1 hour at room temperature. Isotype-matched antibodies to the irrelevant antigen were used in control experiments. Fluorescent images were obtained with a confocal laser fluorescence microscope.

Fluorescein In Situ Hybridization Analysis for the Y-Chromosome

Fluorescein in situ hybridization analysis (FISH) for the Y-chromosome was performed principally according to the published method.[12,20] Briefly, we performed a two-step procedure on 6-μm-thick paraffin-embedded sections: immunostaining with FITC-conjugated anti-CD34 mAb and TO-PRO-3, followed by FISH of the same section using a DNA probe for the Y-chromosome (Vysis, Downers Grove, IL) and restaining with TO-PRO-3. The slides were observed under a confocal laser fluorescence microscope. The fields of the immunostaining and FISH images were matched according to the location and architecture of the tissue, especially the nuclear distribution, to be as close to each other as possible. $CD34^+$ spindle-shaped cells with an oval nucleus residing in the interstitium were regarded as fibroblasts, whereas cells with a single Y-FISH signal in the nucleus were regarded as donor-derived male cells. Three observers blindly evaluated at least 100 nonoverlapping fibroblasts. The frequency (%) of donor-derived fibroblasts was calculated according to the after following formula: the number of $Y\text{-}FISH^+$ fibroblasts divided by the number of fibroblasts. At least three different fields of three to four sections were analyzed by three independent observers and the results expressed as the mean $\pm$ SD. Cultured fibroblasts were also analyzed with a combination of X- and Y-specific probes (Vysis).

In Situ Hybridization for Detection of Male-Specific mRNA

Donor-derived male cells were further detected by in situ hybridization (ISH; GenPoint System; Dako).[21] The *Smcy* gene was used as a male-specific marker,[22] and an antisense probe (5′-TTGTCTTAGTGCAGGGCTCTAGGCTCAAGTGCTGCT-3′) and the corresponding sense probe were labeled with digoxigenin at the 5′ end and incubated with consecutive sections.

Detection of the Y-Chromosome by PCR

Genomic DNA was extracted from freshly isolated cells or cultured cells by proteinase K digestion, followed by phenol extraction and ethanol precipitation. The Y-chromosome-specific *TSPY* gene[23] was amplified by PCR with a sense primer (5′-CTTCCACCTTCAGCCACCGCCTCCTCT-3′) and an antisense primer (5′-CTGTTGTGCGCTGCCTTGACGACCCAG-3′). The PCR condition was 40 cycles of 30 seconds at 95°C, 30 seconds at 66°C, and 1 minute at 72°C.[24] The PCR products were resolved by electrophoresis on 1.5% agarose gels and visualized by staining with ethidium bromide. The PCR procedure was repeated at least two times.

Detection of Mismatched Microsatellite Markers

Microsatellite polymorphic markers were determined by PCR using fluorescein-labeled primers followed by analysis of the length of the products using a capillary automated sequencer (Prism 310; Applied Biosystems, Inc. [ABI], Foster City, CA).[25] The polymorphic microsatellite markers evaluated were *D10S674*, *D10S518*, *D10S466*, *chr10.fa.07frz.20604262*, *AL157895.3_20342*, *D10S595*, *D10S211*, and *D10S1228* on chromosome 10.[25] Mismatched polymorphic mark-

TABLE 1. Demographic and Clinical Characteristics of Patients with Chronic GVHD

Case	Age at Biopsy	Recipient Gender	Donor Gender	Hematopoietic Stem Cell Source	Underlying Disease	Donor Type	TBI	Interval between HSCT and Biopsy (mo)	Interval between Dry Eye Onset and Biopsy (mo)	FS (points)	RB (points)	BUT (seconds)	Degree of Dry eye	Clinically Affected Chronic GVHD Organs
1	32	Female	Male	Bone marrow	APL	Related	+	36	18	3	3	3	Mild	Eye, liver
3	35	Female	Male	Bone marrow	CML	Unrelated	+	14	7	6	5	0	Severe	Eye, mouth, liver, lung, skin
11	22	Female	Male	Bone marrow	APL	Unrelated	+	29	18	5	7	2	Severe	Eye, mouth, liver
13	44	Female	Male	Bone marrow	MDS	Unrelated	+	11	5	6	5	3	Severe	Eye, mouth, intestine, skin
14	39	Female	Male	Peripheral blood	CML	Related	+	13	2	1	3	5	Mild	Eye
16	42	Female	Male	Bone marrow	ALL	Related	+	23	12	5	3	3	Severe	Eye, mouth, liver, lung
17	36	Female	Male	Peripheral blood	MM	Related	−	11	9	3	5	3	Severe	Eye, mouth, liver
15	38	Male	Male	Bone marrow	MDS	Unrelated	+	9	2	3	5	4	Mild	Eye
2	47	Female	Female	Bone marrow	AML	Unrelated	+	5	0	3	3	5	Mild	Eye, liver

APL, acute promyelocytic leukemia; CML, chronic myelogenous leukemia; MDS, myelodysplastic syndrome; ALL, acute lymphoblastic leukemia; MM, multiple myeloma; AML, acute myelogenous leukemia; TBI, total body irradiation; FS, fluorescein score; RB, rose-bengal score; BUT, tear break-up time.

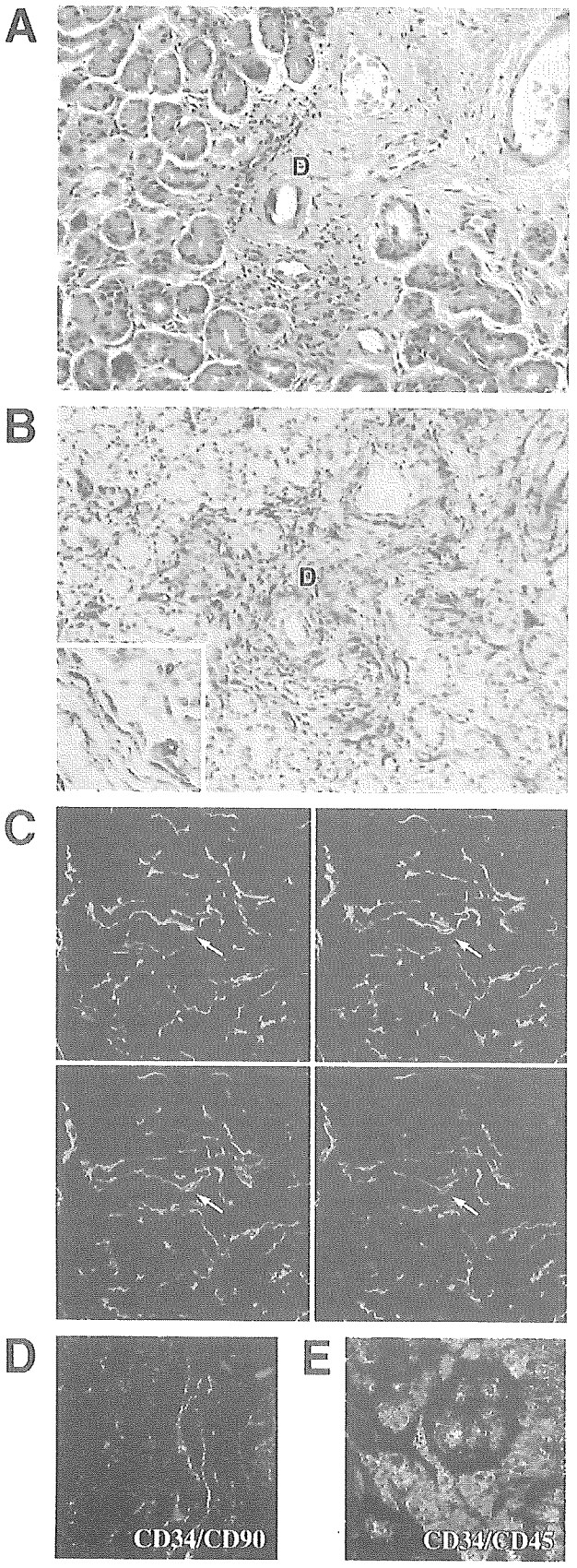

ers were identified by comparing the peaks generated from the samples with those obtained using control donor and recipient-derived cells. All microsatellite analysis was repeated at least two times.

Results

Clinical Characteristics of Patients with Chronic GVHD

Demographic and clinical characteristics of nine HSCT recipients are summarized in Table 1. Allogeneic grafts were derived from the bone marrow in seven patients and from the G-CSF-mobilized peripheral blood in two patients. An interval between HSCT and lacrimal gland biopsy and an interval between onset of dry eye and the biopsy were various among the patients. All patients had symptomatic dry eye and ocular findings typical of chronic GVHD. The degree of dry eye was severe in five patients. Seven patients had additional chronic GVHD lesions in areas such as the mouth, intestine, liver, lung, and skin.

Lacrimal Gland Histology

The lacrimal gland of all the patients represented various degrees of fibrosis in the interstitium and irregular cell loss of the acini with mild lymphocyte infiltration (Fig. 1A). CD34 immunostaining showed marked expression in the periductal interstitium (Fig. 1B). Most $CD34^+$ cells had a spindle-shaped morphology with an oval nucleus, consistent with fibroblasts. Typical *z*-series images for CD34 expression showed that the $CD34^+$ cells had a complex morphology. They were spatially distributed but connected to each other, forming a reticular network (Fig. 1C). CD34 was originally found to be expressed on hematopoietic stem cells and endothelial cells, but was later shown also to be expressed on a subset of stromal fibroblasts in normal exocrine glands.[26] To confirm whether $CD34^+$ cells accumulated in the chronic GVHD lacrimal gland were fibroblasts, we subjected lacrimal gland tissue to double-staining for CD34 in combination with CD90 or CD45. Most $CD34^+$ cells in the interstitium coexpressed a fibroblast marker CD90,[27] but only half of $CD90^+$ fibroblasts expressed CD34 (Fig. 1D), indicating that there were $CD34^+$ and $CD34^-$ fibroblasts in the lacrimal gland from patients with chronic GVHD. In contrast, none of the $CD34^+$ cells simultaneously expressed a hematopoietic marker CD45, whereas many $CD45^+$ round cells were located around spindle-shaped $CD34^+$ cells (Fig. 1E). Taken together, these findings indicate that most $CD34^+$ spindle-shaped cells that accumulate in the interstitium of lacrimal gland are nonhematopoietic fibroblasts.

Detection of Donor-Derived $CD34^+$ Fibroblasts in the Lacrimal Gland Tissue

To evaluate the origin of the fibroblasts that accumulated in the lacrimal gland tissue, we used the Y-chromosome as a

FIGURE 1. Typical histologic findings of the lacrimal gland in patients with chronic GVHD. (**A**) Hematoxylin and eosin staining of a section from patient 14. D, duct. (**B**) CD34 immunostaining of the consecutive section of (**A**). *Inset*: A high-magnification view. (**C**) The *z*-series images of CD34 immunostaining on a 10-μm-thick paraffin-embedded section from patient 13. A series of 1.67-μm optical images is shown. CD34 expression was demonstrated by FITC (*green*), whereas nuclei were counterstained with TO-PRO-3 (*blue*). *Arrows*: one particular $CD34^+$ fibroblast appeared on multiple consecutive sections. (**D**) Immunofluorescent double-staining of CD34 (*green*) and CD90 (*red*) on a lacrimal gland section from patient 17. Nuclei were counterstained with TO-PRO-3 (*blue*). (**E**) Immunofluorescence double-staining of CD34 (*green*) and CD45 (*red*) on a lacrimal gland section from patient 17. Nuclei were counterstained with TO-PRO-3 (*blue*). Original magnification: (**A**, **B**) ×100; (**A**, *inset*) ×400; (**C**–**E**) ×630.

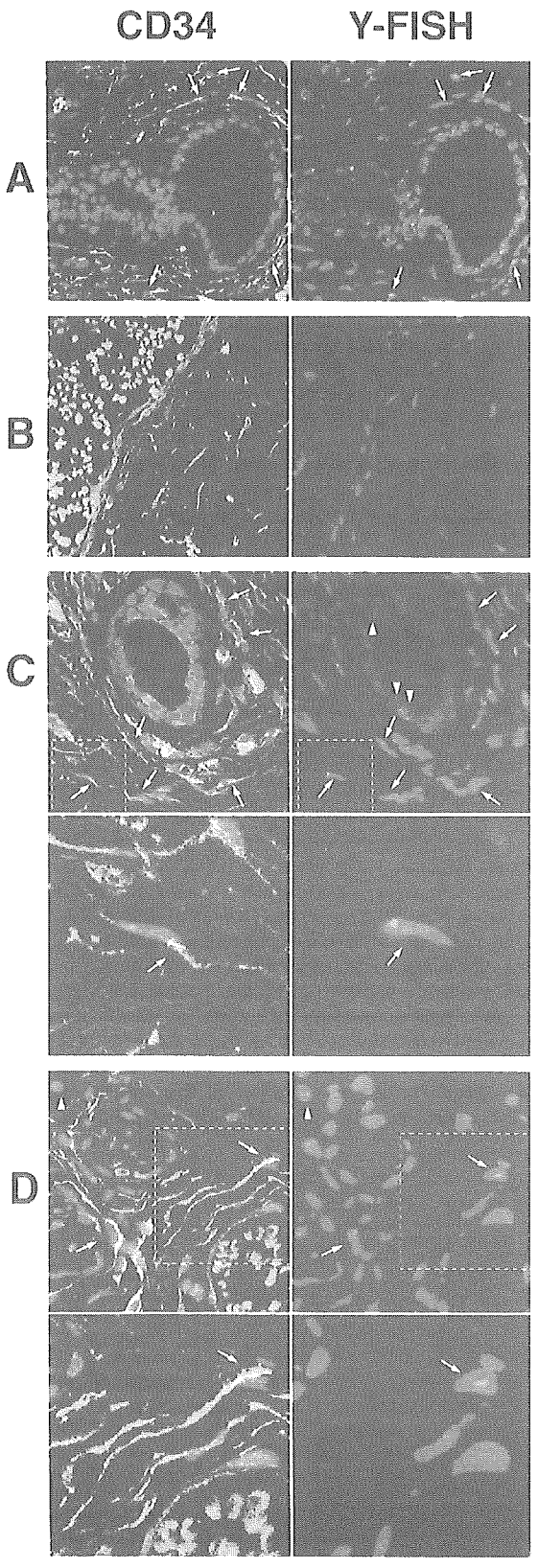

FIGURE 2. Representative CD34 immunostaining and Y-FISH images of the same lacrimal gland sections from patients with chronic GVHD. *Left*: CD34 staining (*green*); *right*: Y-FISH (*red*) with TO-PRO-3 staining (*blue*) of the same region. (**A**) Male-to-male recipient 15. (**B**) Female-to-female recipient 2. (**C**) Male-to-female recipient 17. (**D**) Male-to-female recipient 14. (**C**, **D**, *bottom*) High-magnification views of lesions shown in *dotted squares*. *Arrows*: $CD34^+$ fibroblasts with a Y-FISH signal; *arrowheads*: $Y\text{-}FISH^+$ cells negative for CD34. Red blood cells in the vascular lumen showed nonspecific autofluorescence.

marker for the donor cells in male-to-female recipients. As a marker for fibroblasts, we selected CD34 expressed by most accumulated fibroblasts. We first made sure that our procedure for identifying $Y\text{-}FISH^+$ fibroblasts was reliable by examining positive and negative control cells. Lacrimal gland sections from male-to-male recipient 15 provided the positive control and sections from female-to-female recipient 2 served as the negative control. In sections from the positive control, a Y-FISH signal was detected in nearly half of the nuclei of the $CD34^+$ fibroblasts (Fig. 2A), and the frequency of $Y\text{-}FISH^+$ fibroblasts was 45.2% ± 5.0%. The low sensitivity is probably due to truncation of the Y-chromosome sequence during sectioning and/or incomplete hybridization. The positive frequency of $Y\text{-}FISH^+$ cells in the male tissue was comparable to the value in previous reports.[13,28] In contrast, no Y-FISH signal was detected in the negative control sections (Fig. 2B). We next evaluated lacrimal gland tissue from seven male-to-female recipients. Representative images for CD34 immunostaining and Y-FISH of the same section are shown in Figures 2C and 2D. Donor-derived fibroblasts with a Y-FISH signal were found around medium-sized ducts (Fig. 2C) and blood vessels (Fig. 2D), where the number of fibroblasts was increased. The proportion of donor-derived cells in the $CD34^+$ fibroblasts ranged from 13.4% to 26.7% (Table 2), but this observed frequency was underestimated because the frequency in the male-to-male recipient was only 45.2% ± 5.0%. We also noted $Y\text{-}FISH^+$ donor-derived cells negative for CD34 in the interstitium and in the epithelia of acini and ducts. Most these cells were probably lymphocytes (Fig. 2C and Fig. 2D, arrowheads), but some may have been $CD34^-$ fibroblasts and epithelial cells.

For the seven male-to-female recipients, there was no significant association of the donor-derived fibroblast frequency with the donor type (related versus unrelated), interval between HSCT and biopsy, interval between onset of dry eye and biopsy, the degree of dry eye (severe versus mild), or the presence of other clinically affected chronic GVHD lesions. The frequency of donor-derived $CD34^+$ fibroblasts in patients 16 and 17, who received a transplant of peripheral blood stem cells, was comparable to the frequency in the other patients, who underwent transplantation of bone marrow cells.

We further examined the presence of donor-derived fibroblasts in the lacrimal gland by in situ hybridization for the male-specific *Smcy* gene. To verify the assay system, we evaluated lacrimal gland sections from male-to-male recipient 15 and a female patient with Sjögren's syndrome. As expected, a positive signal was detected for the antisense probe in the male control (Fig. 3A) but not in the female control (Fig. 3B). Representative results of male-to-female recipient 1 showed donor-derived fibroblasts (arrows) and endothelium (arrowheads) in the periductal area (Fig. 3C). The consecutive section incubated with the sense probe showed negative staining. The sections from four additional male-to-female recipients all showed positive staining specific for the antisense probe in the interstitial fibroblasts (Table 2). In consecutive sections from male-to-female recipient 17, *Smcy*-positive fibroblasts around a

TABLE 2. Identification of Donor-Derived Fibroblasts in the Chronic GVHD Lacrimal Gland Tissue

Case	Gender of Donor and Recipient	%Y-FISH$^+$ CD34$^+$ Fibroblasts*	Y-Chromosome$^+$ Fibroblasts by ISH
1	Male-to-female	13.4 ± 2.9	Present
3	Male-to-female	26.7 ± 9.4	Present
11	Male-to-female	20.0 ± 0.0	Not tested
13	Male-to-female	13.4 ± 1.2	Present
14	Male-to-female	20.1 ± 3.0	Present
16	Male-to-female	17.2 ± 6.8	Not tested
17	Male-to-female	14.7 ± 2.5	Present
15	Male-to-male	45.2 ± 5.0	Present
2	Female-to-female	0	Absent

* The mean ± SD of three independent observations of more than 100 fibroblasts.

medium-sized duct were confirmed to be positive for CD34 and Y-FISH signals (Fig. 3D).

Detection of Donor-Derived Cells in Primary Fibroblast Cultures Generated from Lacrimal Gland Biopsy Specimens

Primary fibroblast cultures generated from lacrimal gland biopsies were used as a source material for confirmation of the presence of donor-derived fibroblasts. This primary culture was successfully generated from four patients with chronic GVHD, including three male-to-female recipients and one male-to-male recipient (Table 3). All the cells in these cultures had a spindle shape and were positive for vimentin, collagen type I, and CD90 (Fig. 4A), consistent with the fibroblast phenotype. None of the cells were positive for CD45, cytokeratin, or factor VIII, indicating no contamination by cells of hematopoietic, endothelial, or epithelial origin. The cultured fibroblasts were heterogeneous in terms of CD34 expression (Fig. 4A), and the proportion of CD34$^+$ cells ranged from 40% to 88% at the fifth passage in the cultures from four patients.

FISH was performed on cultured fibroblasts with probes for X- and Y-chromosomes (Fig. 4B). The culture from male-to-male recipient 15 showed that the detection sensitivity of cells positive for a set of X- and Y-FISH signals was 50%. In contrast, control dermal fibroblasts generated from a female individual exhibited one or two X-FISH signals and no Y-FISH signal in all cells. In two male-to-female recipients (patients 16 and 17), the frequency of donor-derived fibroblasts with a set of X- and Y-FISH signals in a total of 200 cells was 2% and 4%, respectively. The frequency of donor-derived fibroblasts in the primary culture was much lower than that observed in the tissue, probably because of the predominance of the residential fibroblasts of recipient origin that had grown in the in vitro culture. When Y-FISH was combined with CD34 immunostaining, donor-derived fibroblasts were detected in both CD34$^+$ and CD34$^-$ cell populations (data not shown). In situ hybridization for the *Smcy* antisense probe also demonstrated the presence of donor-derived fibroblasts in male-to-female recipient 17.

Genomic DNA was extracted from the cultured fibroblasts and used in assays to detect genetic markers that are different between recipients and donors. First, the Y-chromosome-specific *TSPY* gene was used as a marker for male cells in PCR. In a representative male-to-female recipient, patient 14, the *TSPY* gene was not amplified in the recipient before HSCT BCL, but was amplified in cultured lacrimal gland fibroblasts obtained after HSCT, donor peripheral blood and bone marrow cells, and post-HSCT recipient BCL (Fig. 4C). Analogous findings were obtained in two additional male-to-female recipients (patients 16 and 17).

Microsatellite markers were also used to test for a chimeric status based on variation in the length of the PCR products (Fig. 4D). In male-to-female recipient 14, lacrimal

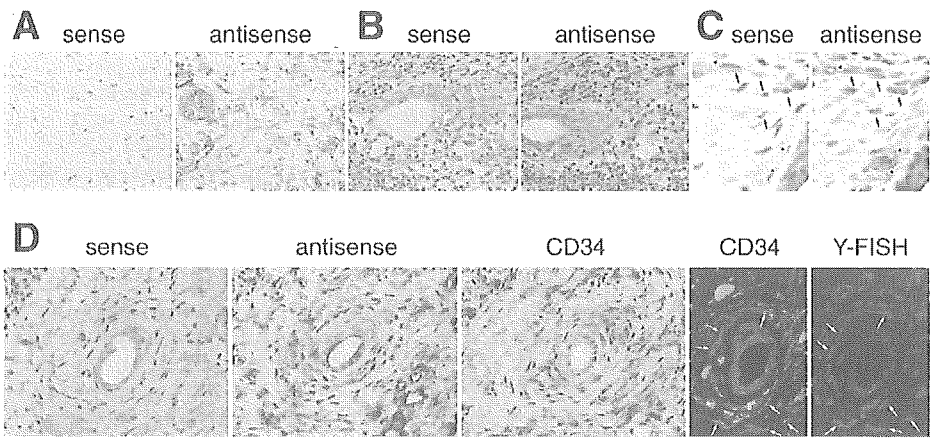

FIGURE 3. In situ hybridization for the detection of Y-chromosome-specific *Smcy* mRNA in lacrimal gland tissue sections from patients with chronic GVHD. Consecutive sections using sense and antisense probes are shown for individual specimens. (**A**) Male-to-male recipient 15. (**B**) A female patient with Sjögren's syndrome. (**C**) Male-to-female recipient 1 (diaminobenzidine staining). *Arrows*: donor-derived fibroblasts positive for the antisense signal; *arrowhead*: donor-derived endothelia of the small vessel. (**D**) Consecutive sections from male-to-female recipient 17 (immunofluorescent staining) that were subjected to in situ hybridization for *Smcy* mRNA, diaminobenzidine immunostaining for CD34, fluorescent immunostaining for CD34, and Y-FISH. Fluorescent immunostaining for CD34 and Y-FISH were performed on a single section. *Arrows*: CD34$^+$ fibroblasts with a Y-FISH signal. Original magnification: (**A**, **B**, **D**) ×200, (**C**, diaminobenzidine staining) ×400; (**D**, immunofluorescent staining) ×630.

TABLE 3. Identification of Donor-Derived Cells in Fibroblast Primary Cultures Derived from the Lacrimal Gland in Chronic GVHD

Case	Gender of Donor and Recipient	% Y-FISH$^+$ Fibroblasts*	Y-Chromosome$^+$ Fibroblasts by ISH	Y-chromosome$^+$ Fibroblasts by Y-PCR	Mismatched Microsatellite Markers†
14	Male-to-female	Not tested	Present	Present	1/8
16	Male-to-female	2	Not tested	Present	1/8
17	Male-to-female	4	Present	Present	0/8
15	Male-to-male	50	Present	Present	3/3

Y-PCR, Y-chromosome polymerase-chain reaction.

* Frequency of cells positive for both X- and Y-FISH signals in 200 cultured cells.

† The number of microsatellite markers mismatched between donor and recipient divided by the total number of markers examined.

gland fibroblasts displayed a combination of the recipient pattern observed in the recipient before HSCT BCL and the donor pattern observed in the donor peripheral blood mononuclear cells and bone marrow cells as well as in the recipient after HSCT BCL. The donor-specific peak in cultured lacrimal gland fibroblasts was lower than the recipient-specific and shared peaks, due to a low abundance of donor-derived cells in the cultured fibroblasts. Theoretically, this method should allow us to detect donor-derived cells in cultured fibroblasts, irrespective of the combination of donor-recipient genders. In fact, a combination of the donor and recipient peaks was detected in the cultured lacrimal gland fibroblasts derived from male-to-male recipient 15. Analogous findings were obtained in an additional recipient 16, but no donor-recipient-mismatch marker was detected among the markers used in another recipient (patient 17).

DISCUSSION

In this study, the chimeric status of accumulated CD34$^+$ fibroblasts in the lacrimal gland of chronic GVHD patients was clearly demonstrated by a series of experiments using lacrimal gland tissue specimens and lacrimal gland-derived cultured fibroblasts. Nearly half of the CD34$^+$ fibroblasts at the site of pathogenic fibrosis were of donor origin, and the proportion of donor-derived cells in the fibrotic chronic GVHD lesion is considerably higher than the proportions reported for other donor-derived nonhematopoietic cells engrafted in tissues of HSCT recipients.[10–14] Although both CD34$^+$ and CD34$^-$ fibroblasts accumulate in the lacrimal gland from patients with chronic GVHD, we had to use CD34 as a marker for fibroblasts because there is no reliable fibroblast marker that can be used in the tissue. This limitation should be considered on interpreting our findings. In addition, there are several other limitations in our study for ethical reasons. The study lacks specimens from non-GVHD transplant recipient control subjects and serial specimens for evaluating a potential association between influx of donor-derived fibroblasts and disease progression. The role of donor-derived fibroblasts in the pathogenesis of chronic GVHD should be further examined in animal models.

Recent studies suggest that hematopoietic stem cells may spontaneously fuse with other cells and give the appearance of differentiation.[29,30] In this regard, Tran et al.[14] reported that more than 9700 buccal epithelial cells obtained from HSCT recipients showed no evidence of fusion, with only a few exceptions, indicating that cell fusion is a rare event in vivo in humans. Given the relatively high frequency of donor-derived CD34$^+$ fibroblasts in the chronic GVHD lacrimal gland, the fusion of donor-derived hematopoietic cells with residential fibroblasts was unlikely, although we could not entirely exclude the possibility that cell fusion was partly responsible for our observations.

Although the donor-derived fibroblasts that accumulate in the lacrimal gland chronic GVHD lesions apparently originated from the transplanted donor bone marrow or mobilized peripheral blood cells, the precise origin of these cells is presently unknown. The potential cell source includes mesenchymal stem cells with a capacity for self renewal and the potential to give rise to the various mesenchymal cells identified in human bone marrow,[31] but whether such stem cells circulate in the blood is not known. In fact, two patients with the significant chimeric status of fibroblasts in the lacrimal gland received transplantation of peripheral blood cells. Alternatively, donor stem cells that are committed to differentiation primarily along the hematopoietic lineage may switch to the fibroblast lineage under the influence of signals from the local environment. In this regard, mesenchymal cells can be differentiated from a distinct hematopoietic lineage termed fibrocytes[15] and from circulating monocytes.[32]

Our findings address important questions in the pathogenesis of chronic GVHD. It was originally considered to be a later phase of acute GVHD due to allorecognition by donor T cells, but several recent studies suggest that an autoimmune-like process induced by dysfunctional immunologic recovery also plays some roles.[1] In addition, the fibrotic process is apparently accelerated and the resultant excessive fibrosis leads to functional impairment in various organs, including the lacrimal glands.[8] Our findings suggest that donor-derived fibroblasts may be involved in this process. It has been postulated that, in HSCT recipients, tissue injury caused by acute GVHD, a conditioning regimen, or in some other way facilitates the homing of circulating stem cells or precursors and their differentiation into various tissues under the signals of the local environment.[33] Therefore, it is likely that the persistent fibrotic environment in chronic inflammatory lesions promotes the recruitment and mobilization of donor-derived fibroblast precursors, which may have unlimited growth potential or may be constantly supplied from the circulation in chronic GVHD. This possibility is supported by a murine sclerodermatous GVHD showing massive fibrosis, in which infiltration of macrophages and T cells into the tissue preceded fibrosis in the skin and lung.[34] Because no specific treatment has been shown to be effective for lacrimal gland chronic GVHD, strategies that inhibit the recruitment of fibroblast precursors into the affected lesion could be a novel therapeutic

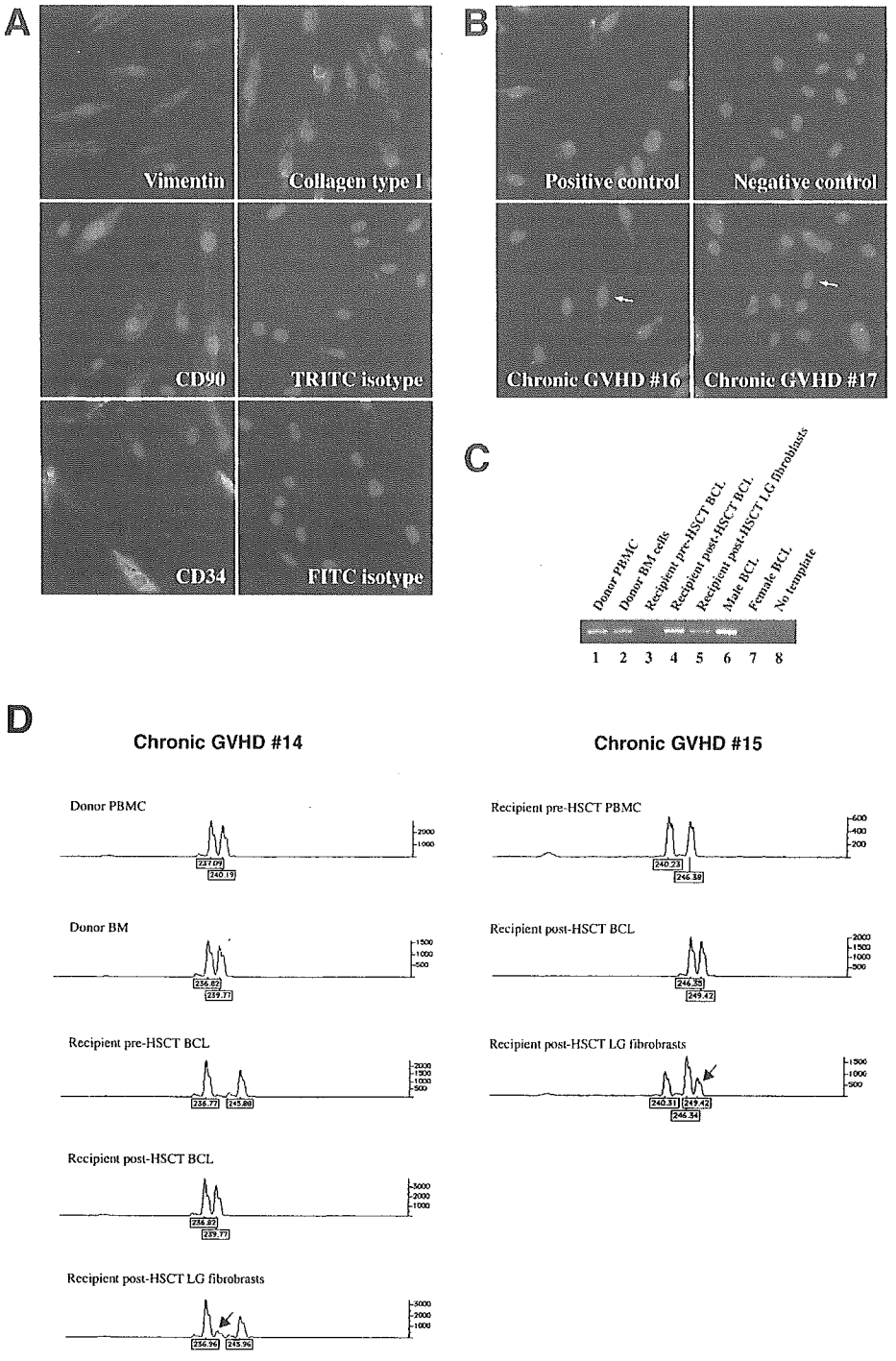

FIGURE 4. Detection of donor-derived cells in primary fibroblast cultures generated from the lacrimal gland of patients with chronic GVHD. (**A**) Cultured fibroblasts derived from patient 17 were stained for vimentin, collagen type I, CD90 (TRITC; *red*), and CD34 (FITC; *green*). Isotype-matched control mAbs to irrelevant antigens were used instead of the primary mAb as isotype controls. Nuclei were counterstained with TO-PRO-3 (*blue*). (**B**) FISH for the Y (*red*)- and X (*green*)-chromosome with TO-PRO-3 staining (*blue*). Cultured fibroblasts from male-to-male recipient 15 were used as the positive control, whereas dermal fibroblasts from a female subject were used as the negative control. Results obtained from male-to-female recipients 16 and 17 are shown. *Arrows*: fibroblasts with both X- and Y-FISH signals. (**C**) PCR for the detection of the Y-chromosome-specific *TSPY* gene in various cell sources obtained from male-to-female recipient 14 and her related donor before and after HSCT. *Lane 1*: donor PBMC; *lane 2*: donor bone marrow (BM) cells; *lane 3*, recipient pre-HSCT BCL; *lane 4*, recipient post-HSCT BCL; *lane 5*, recipient post-HSCT lacrimal gland (LG) fibroblasts; *lane 6*, male BCL as the positive control; *lane 7*, female BCL as the negative control; and *lane 8*, no-template DNA. (**D**) The analysis of polymorphic microsatellite marker *D10S1228* in various cell sources obtained from male-to-female recipient 14 and male-to-male recipient 15 before and after HSCT. The *x*- and *y*-axes show the product length in bases and signal strength, respectively. *Arrows*: indicate the donor-specific peak detected in the recipient peak pattern. Original magnification: (**A**, **B**) ×400.

approach to the fibrotic process in lacrimal gland chronic GVHD.

It has been shown recently that bone-marrow-derived precursors can serve as a source for fibroblasts in a mouse model of pulmonary fibrosis.[16] Our study demonstrates, for the first time, the presence of bone-marrow-derived fibroblasts in pathogenic fibrosis of the human disease. This finding leads us to propose a hypothesis that bone-marrow-derived fibroblasts may contribute to the pathogenesis of human fibrotic diseases, such as pulmonary fibrosis, cirrhosis of the liver, scleroderma, and ocular cicatricial pemphigoid. It would be interesting to evaluate further the chimeric status in multiple chronic GVHD tissues and potential associations between the chimeric status and response to various therapeutic regimens.

Acknowledgments

The authors thank Eri Kikkawa for assistance in microsatellite analysis, Rie Yamazaki for collecting the patients' samples, and Takashi Mamizuka and Takahiro Tsuda for expert technical assistance.

References

1. Sullivan KM. Graft-vs.-host disease. In: Blume KG, Forman SJ, Applebaum FR, eds. *Thomas' Hematopoietic Cell Transplantation.* 3rd ed. Malden, MA: Blackwell; 2004:635-664.
2. Ferrara JLM, Antin J. The pathophysiology of graft-vs.-host disease. In: Blume KG, Forman SJ, Applebaum FR, eds. *Thomas' Hematopoietic Cell Transplantation.* 3rd ed. Malden, MA: Blackwell; 2004:353-368.
3. Sale GE, Shulman HM, Hackman RC. Pathology of hematopoietic cell transplantation. In: Blume KG, Forman SJ, Applebaum FR, eds. *Thomas' Hematopoietic Cell Transplantation.* 3rd ed. Malden, MA: Blackwell; 2004:286-299.
4. Vogelsang GB, Lee L, Bensen-Kennedy DM. Pathogenesis and treatment of graft-versus-host disease after bone marrow transplant. *Annu Rev Med.* 2003;54:29-52.
5. Mencucci R, Ferrini CR, Bosi A, Volpe R, Guidi S, Salvi G. Ophthalmological aspects in allogeneic bone marrow transplantation: Sjögren-like syndrome in graft-versus-host disease. *Eur J Ophthalmol.* 1997;7:13-18.
6. Tichelli A, Duell T, Weiss M, et al. Late-onset keratoconjunctivitis sicca syndrome after bone marrow transplantation: Incidence and risk factors. *Bone Marrow Transplant.* 1996;17:1105-1111.
7. Ogawa Y, Okamoto S, Wakui M, et al. Dry eye after haematopoietic stem cell transplantation. *Br J Ophthalmol.* 1999;83:1125-1130.
8. Ogawa Y, Yamazaki K, Kuwana M, et al. A significant role of stromal fibroblasts in rapidly progressive dry eye in patients with chronic GVHD. *Invest Ophthalmol Vis Sci.* 2001;42:111-119.
9. Ogawa Y, Kuwana M, Yamazaki K, et al. Periductal area as the primary site for T-cell activation in lacrimal gland chronic graft-versus-host disease. *Invest Ophthalmol Vis Sci.* 2003;44:1888-1896.
10. Mezey E, Key S, Vogelsang G, et al. Transplanted bone marrow generates new neurons in human brains. *Proc Natl Acad Sci USA.* 2003;100:1364-1369.
11. Okamoto R, Yajima T, Yamazaki M, et al. Damaged epithelia regenerated by bone marrow-derived cells in the human gastrointestinal tract. *Nat Med.* 2002;8:1011-1017.
12. Körbling M, Katz RL, Khanna A, et al. Hepatocytes and epithelial cells of donor origin in recipients of peripheral-blood stem cells. *N Engl J Med.* 2002;346:738-746.
13. Brittan M, Hunt T, Jeffery R, et al. Bone marrow derivation of pericryptal myofibroblasts in the mouse and human small intestine and colon. *Gut.* 2002;50:752-757.
14. Tran SD, Pillemer SR, Dutra A, et al. Differentiation of human bone marrow-derived cells into buccal epithelial cells in vivo: a molecular analytical study. *Lancet.* 2003;361:1084-1088.
15. Bucala R, Spiegel LA, Chesney J, Hogan M, Cerami A. Circulating fibrocytes define a new leukocyte subpopulation that mediates tissue repair. *Mol Med.* 1994;1:71-81.
16. Hashimoto N, Jin H, Liu T, Chensue SW, Phan SH. Bone marrow-derived progenitor cells in pulmonary fibrosis. *J Clin Invest.* 2004;113:243-252.
17. Lemp MA. Report of the National Eye Institute/Industry Workshop on clinical trials on dry eye. *CLAO J.* 1995;21:221-232.
18. Shulman HM, Sullivan KM, Weiden PL, et al. Chronic graft-versus-host syndrome in man: a long-term clinicopathologic study of 20 Seattle patients. *Am J Med.* 1980;69:204-217.
19. Tsubota K. The importance of Schirmer test with nasal stimulation test. *Am J Ophthalmol.* 1991;111:106-108.
20. Shimazaki J, Kaido M, Shinozaki N, et al. Evidence of long-term survival of donor-derived cells after limbal allograft transplantation. *Invest Ophthalmol Vis Sci.* 1999;40:1664-1668.
21. Kodama H, Hirotani T, Suzuki Y, Ogawa S, Yamazaki K. Cardiomyogenic differentiation in cardiac myxoma expressing lineage-specific transcription factors. *Am J Pathol.* 2002;161:381-389.
22. Agulnik AI, Mitchell MJ, Lerner JL, Woods DR, Bishop CE. A mouse Y chromosome gene encoded by a region essential for spermatogenesis and expression of male-specific minor histocompatibility antigens. *Hum Mol Genet.* 1994;3:873-878.
23. Vogel T, Schmidtke J. Structure and function of TSPY, the Y-chromosome gene coding for the "testis-specific protein." *Cytogenet Cell Genet.* 1998;80:209-213.
24. Toda I, Kuwana M, Tsubota K, Kawakami Y. Lack of evidence for an increased microchimerism in the circulation of patients with Sjögren's syndrome. *Ann Rheum Dis.* 2001;60:248-253.
25. Savoia A, Del Vecchio M, Totaro A, et al. An autosomal dominant thrombocytopenia gene maps to chromosomal region 10p. *Am J Hum Genet.* 1999;65:1401-1405.
26. Yamazaki K, Eyden BP. Ultrastructural and immunohistochemical studies of intralobular fibroblasts in human submandibular gland: the recognition of a CD34 positive reticular 'network' connected by gap junctions. *J Submicrosc Cytol Pathol.* 1996;28:471-483.
27. Saalbach A, Kraft R, Herrmann K, Haustein UF, Anderegg U. The monoclonal antibody AS02 recognizes a protein on human fibroblasts being highly homologous to Thy-1. *Arch Dermatol Res.* 1998;290:360-366.
28. Deb A, Wang S, Skelding KA, et al. Bone marrow-derived cardiomyocytes are present in adult human heart: a study of gender-mismatched bone marrow transplantation patients. *Circulation.* 2003;107:1247-1249.
29. Terada N, Hamazaki T, Oka M, et al. Bone marrow cells adopt the phenotype of other cells by spontaneous cell fusion. *Nature.* 2002;416:542-545.
30. Ying QL, Nichols J, Evans EP, et al. Changing potency by spontaneous fusion. *Nature.* 2002;416:545-548.
31. Pittenger MF, Mackay AM, Beck SC, et al. Multilineage potential of adult human mesenchymal stem cells. *Science.* 1999;284:143-147.
32. Kuwana M, Okazaki Y, Kodama H, et al. Human circulating $CD14^+$ monocytes as a source of progenitors that exhibit mesenchymal cell differentiation. *J Leukoc Biol.* 2003;74:833-845.
33. Anderson DJ, Gage FH, Weissman IL. Can stem cells cross lineage boundaries? *Nat Med.* 2001;7:393-395.
34. Zhang Y, McCormick LL, Desai SR, Wu C, Gilliam AC. Murine sclerodermatous graft-versus-host disease, a model for human scleroderma: cutaneous cytokines, chemokines, and immune cell activation. *J Immunol.* 2002;168:3088-3098.

ELSEVIER

Journal of Neuroimmunology 170 (2005) 141 – 149

Journal of
Neuroimmunology

www.elsevier.com/locate/jneuroim

Novel autoantibodies to a voltage-gated potassium channel $K_V1.4$ in a severe form of myasthenia gravis

Shigeaki Suzuki [a,b], Takashi Satoh [b], Hidekata Yasuoka [c], Yasuhito Hamaguchi [d], Kortaro Tanaka [a], Yutaka Kawakami [b], Norihiro Suzuki [a], Masataka Kuwana [b,*]

[a] *Department of Neurology, Keio University School of Medicine, 35 Shinanomachi, Shinjuku-ku, Tokyo 160-8582, Japan*
[b] *Institute for Advanced Medical Research, Keio University School of Medicine, 35 Shinanomachi, Shinjuku-ku, Tokyo 160-8582, Japan*
[c] *Department of Internal Medicine, Keio University School of Medicine, 35 Shinanomachi, Shinjuku-ku, Tokyo 160-8582, Japan*
[d] *Department of Dermatology, Kanazawa University Graduate School of Medical Science, 13-1 Takaramachi, Kanazawa 920-8640, Japan*

Received 4 April 2005; accepted 17 August 2005

Abstract

Sera from patients with myasthenia gravis (MG) were screened for autoantibodies to skeletal muscle-specific antigens by immunoprecipitation assay, using rhabdomyosarcoma and leukemia cell lines. Eleven of 61 MG sera immunoprecipitated a rhabdomyosarcoma-specific 70-kDa protein, which was identified as the voltage-gated K^+ channel 1.4 ($K_V1.4$). This antibody specificity was not detected in 30 patients with polymyositis/dermatomyositis, 9 with thymoma alone, or 30 healthy controls. Clinical features associated with anti-$K_V1.4$ antibody included bulbar involvement, myasthenic crisis, thymoma, myocarditis, and QT prolongation on electrocardiogram. These findings suggest that anti-$K_V1.4$ antibody is a novel autoantibody associated with a severe MG subset and thymoma.

Keywords: Autoantibodies; Immunoprecipitation; Myasthenia gravis; Voltage-gated potassium channel

1. Introduction

Myasthenia gravis (MG) is an organ-specific autoimmune disorder characterized by dysfunctional neuromuscular junctions (Drachman, 1994). Autoantibodies to the nicotinic acetylcholine receptor (AChR) are detected in 80–90% of MG patients, and are thought to play a primary role in the pathogenesis of MG. The anti-AChR antibody is specific to MG, and thus used as a diagnostic marker in clinical settings. MG is heterogeneous in terms of its disease expression, ranging from an ocular form to a generalized form requiring intensive immunosuppressive treatment, but the serum concentration of the anti-AChR antibody does not always correlate with the disease severity (Drachman, 1994). This could be because the conventional radioimmunoassay used for detecting anti-AChR antibodies does not adequately quantify the antibodies with pathogenic activity. Another possibility is that additional antibodies that modify the pathogenic process are present in MG patients. In this regard, autoantibodies against proteins that are highly expressed in the skeletal muscle, such as titin and ryanodine receptor, have been detected in MG sera in conjunction with anti-AChR antibodies (Williams and Lennon, 1986; Aarli et al., 1990; Mygland et al., 1992). Moreover, autoantibodies to the receptor tyrosine kinase MuSK were found in patients with seronegative MG (Hoch et al., 2001). The measurement of anti-titin antibodies is reported to have limited clinical use in predicting the presence of thymoma in MG patients below age 60 (Buckley et al., 2001), but the clinical associations of these MG-related autoantibodies are generally weak (Drachman, 1994; Buckley et al., 2001).

To identify additional skeletal muscle-specific autoantibodies in MG sera, we applied an immunoprecipitation

* Corresponding author. Tel.: +81 3 3350 3567; fax: +81 3 3350 3567.
E-mail address: kuwanam@sc.itc.keio.ac.jp (M. Kuwana).

0165-5728/$ - see front matter © 2005 Elsevier B.V. All rights reserved.
doi:10.1016/j.jneuroim.2005.08.017

assay using radiolabeled cellular extracts; this assay is highly sensitive and can detect autoantibodies to a broad range of cellular components in their native conformation (Mimori et al., 1984). The rhabdomyosarcoma cell line RD and leukemia cell line K562 were used as antigen sources, and profiles of the proteins immunoprecipitated by MG sera were compared between assays using these two different cell sources. The proteins immunoprecipitated from the RD extracts, but not from the K562 extracts, were regarded as potential skeletal muscle-specific autoantigens. Using this system, we identified a novel autoantibody to $K_V1.4$, one of the α-subunits of voltage-gated K^+ (K_V) channels, in the sera from MG patients. We further examined the clinical associations of the anti-$K_V1.4$ antibody and the expression of $K_V1.4$ in various human tissues, including abnormal thymus from MG patients.

2. Material and methods

2.1. Patients and controls

We studied serum samples from 61 patients with MG (25 males and 36 females) who were followed at Keio University Hospital, Tokyo, Japan. The diagnosis of MG was based on clinical, electrophysiologic, and immunologic criteria (Drachman, 1994). The mean age at disease onset was 43.9±19.2 years and the mean disease duration at examination was 8.7±5.5 years. Ocular MG was diagnosed in 20 of the patients, and the remaining 41 patients had generalized MG. The MG severity was graded according to the Task Force of the Medical Advisory Board of the Myasthenia Gravis Foundation of America (Jaretzki et al., 2000). Trans-sternal extended thymectomy was performed in 34 patients, and histopathologic examination revealed one normal thymus, 12 cases of thymic hyperplasia, and 21 cases of thymoma. Serum anti-AChR antibody was quantitatively measured by a conventional radioimmunoassay (Drachman, 1994). Fifty-four patients (88%) were positive for anti-AChR antibody at least once during the disease course (range 0.7–440 nM) and the remaining 7 were seronegative. Serum samples were obtained from all MG patients within one year after first visit when their disease was active, and 29 sera were obtained after thymectomy. Clinical information was retrospectively obtained on all MG patients by reviewing their clinical charts. An electrocardiogram was recorded for 56 patients, and the findings were blindly evaluated by cardiologists (Braunwald et al., 2001). Two groups of sera were used as disease controls: sera from 30 patients with definite polymyositis or dermatomyositis (PM/DM), who satisfied the criteria proposed by Bohan and Peter (1975), as a control for autoimmune disease affecting the skeletal muscle; and sera from 9 patients with thymoma, but without MG (2 had pure red cell aplasia, but none had acquired neuromyotonia), as a control for thymoma which is frequently accompanied by MG. Sera from 30 healthy volunteers were also used as a control. All blood samples and clinical information were collected after the patients and controls gave their written informed consent as approved by the Keio University Institutional Review Boards.

2.2. Immunoprecipitation assay using radiolabeled cellular extracts

Serum autoantibodies were detected by immunoprecipitation assay using ^{35}S-labeled cellular extracts as reported previously (Kuwana et al., 1993) with some modifications. Two cultured cell lines, RD and K562, were used as sources for total cellular extracts. In brief, RD and K562 cells (5×10^6 and 10^7 per sample, respectively) were cultured in methionine-free DMEM (Sigma, St. Louis, MO) containing 3% heat-inactivated fetal bovine serum in the presence of 20 μCi/ml ^{35}S-methionine for 14 h. The ^{35}S-labeled cells were resuspended in an ice-cold buffer containing 500 mM NaCl, 0.1% Nonidet P-40, 10 mM Tris–HCl, pH 8.0 (IP buffer) in the presence of a cocktail of protease inhibitors (COMPLETE; Roche, Mannheim, Germany), and sonicated intermittently on ice for a total of 90 s. The supernatant, containing ^{35}S-labeled soluble proteins originating from the nuclei, cytoplasm, and cellular membrane, was recovered by centrifugation (14,000 *g* for 15 min) and used as the antigen source. Two milligrams of protein A-Sepharose CL-4B (Pharmacia Biotech, Stockholm, Sweden) was incubated with 10 μl of a human serum sample in 500 μl of IP buffer for 14 h. The immunoglobulins that were bound to protein A-Sepharose beads were then incubated with the ^{35}S-labeled cellular extracts for 2 h. The immunoprecipitated material was resolved by electrophoresis on SDS-8.5% polyacrylamide gels, which were subsequently treated with 0.5 M sodium salicylate to enhance the radioactivity, dried for 1 h with a gel dryer (Biorad Laboratories, Philadelphia, PA), and evaluated by autoradiography using the BAS-5000 system (Fuji film, Tokyo, Japan). The gels were exposed to the film for 24 h (short exposure) and then for 72 h (long exposure). Immunoprecipitated protein bands were compared between the assays using extracts derived from RD and K562 cells, and the proteins precipitated from the RD extracts, but not from the K562 extracts, were regarded as skeletal muscle-specific autoantigens.

2.3. Affinity-purification of skeletal muscle-specific autoantigens

The antigens recognized by patients' sera were isolated from the RD extracts by affinity-purification as described previously (Kuwana et al., 1999). Briefly, a mixture of MG sera containing the antibody of interest (1 ml) was incubated with protein A-Sepharose CL-4B (1 g), and the antibody–protein A complex was cross-linked by treatment with dimethylpimelimidate (Pierce, Rockford, IL). The cellular extracts derived from RD cells (5×10^8) were incubated with the antibody–protein A bead complex, and proteins

that bound to the antibodies were eluted using a buffer containing 3 M $MgCl_2$ and 1 mM DTT. The eluted materials were dialyzed against PBS, concentrated using an Ultrafree-4 Centrifugal Filter (Millipore, Billerica, MA), and fractionated on SDS-8.5% polyacrylamide gels, followed by Coomassie blue staining. The protein band of interest was cut out from the gel and subjected to N-terminal amino acid sequencing using a protein sequencer, HPG1005A (Hewlett-Packard, Palo Alto, CA) (Masiarz and Malcolm, 1994). The amino acid sequence was subjected to a BLAST search (http://www.ncbi.nlm.nih.gov) of the National Center for Biotechnology Information (NCBI). The molecular weight, isoelectric point (PI), and signal peptide sequence of the protein of interest were predicted using Genetyx-Mac software (Software Development, Tokyo, Japan).

2.4. Determination of PI

The affinity-purified preparation was subjected to 2-dimensional electrophoresis using the ZOOMIPG Runner™ System (Invitrogen, Carlsbad, CA) (Scheele, 1975). Briefly, the samples were applied to ZOOM strips containing a fixed pH gradient, in which individual proteins were immobilized as they approached their PI. In the second dimension of polyacrylamide gel electrophoresis, the proteins were separated based on their molecular weights, followed by silver staining (Silver Stain Plus, Biorad Laboratories).

2.5. Immunoblots

Antigenicity of the affinity-purified preparation was examined by immunoblotting as described (Kuwana et al., 2002). The protein preparation was fractionated on SDS-10% polyacrylamide gels and the proteins were transferred to nitrocellulose membranes. An edge of the membrane was stained with amino black, and the remaining portion was blocked with 5% non-fat milk and incubated with serum samples diluted 1:250, rabbit anti-rat $K_V1.4$ polyclonal antibodies diluted 1:200 (Sigma) (Veh et al., 1995), or rabbit polyclonal antibodies to an irrelevant antigen as a control. The membranes were subsequently incubated with alkaline phosphatase-conjugated goat anti-human or anti-rabbit IgG (Cappel, Aurora, OH), and the immunoreactive bands were visualized by development with 4-nitro blue tetrazolium chloride/5-bromo-4-chloro-3-indolyl-phosphate.

2.6. Indirect immunofluorescence on cells undergoing $K_V1.4$ gene transfer

Total RNA was isolated from RD cells using an RNeasy™ kit (QIAGEN, Valencia, CA), and subjected to reverse transcription with an oligo $(dT)_{12-15}$ primer using AMV reverse-transcriptase XL (Takara, Kusatsu, Japan). A first-strand cDNA encoding the entire open reading frame of human $K_V1.4$ was amplified by PCR and subcloned into a pcDNA3.1 expression vector (Invitrogen) (Philipson et al., 1990). The primer set used was 5′-CTTAAGGGTTCCAAACTTACC-3′ (sense) and 5′-TGCCAACTTTTCCCTTCA-3′ (antisense). Mouse L cells grown on fibronectin-coated chamber slides (Becton Dickinson Labware, Bedford, MA) were transiently transfected with pcDNA3.1 harboring $K_V1.4$ or with empty plasmid, using Effectene reagent (Qiagen, Hilden, Germany). After a 24-h culture in MEM (Sigma) containing 10% FBS, the cells were fixed with 4% paraformaldehyde for 5 min. The cells were then incubated with serum samples diluted 1:20, rabbit anti-rat $K_V1.4$ polyclonal antibodies diluted 1:100, or control rabbit antibodies. All serum samples were pretreated with untransfected mouse L cells to eliminate non-specific antibody binding. After incubation with Alexa Fluor 488-conjugated anti-human IgG and Alexa Fluor 568-conjugated anti-rabbit IgG (Molecular Probes, Eugene, OR), the slides were mounted and examined with a confocal laser fluorescent microscope, LSM5 PASCAL (Carl-Zeiss, Göttingen, Germany).

2.7. Detection of K_V mRNA expression

The mRNA expression of $K_V1.4$ and other K_V channels was examined in various cell lines and human tissues using reverse transcription combined with PCR. The expression of GAPDH mRNA was also examined, as a house-keeping gene control. The primary skeletal myoblast culture was established from a skeletal muscle biopsy specimen from an individual with histologically normal muscle. The thymus tissue was obtained from MG patients who received extended thymectomy or autopsy. Total RNA samples obtained from a panel of normal human tissues were purchased from Clontech (Palo Alto, CA). Each cDNA (12.5 ng total RNA equivalent) was subjected to PCR as a template. The primer sets used were as follows: $K_V1.4$ (sense, 5′-CAGCACCCCATCTGGAGAAC-3′ and antisense, 5′-CTGGGATGCTTTGGAAATGGG-3′), $K_V1.3$/1.5/1.6 (sense, 5′-TTCCAGCGCCAGGTGTGGC-3′ and antisense, 5′-CTGCAGCCCCTTGGAGTGGCG-3′) (Liyanage et al., 1998), $K_V4.2$ (sense, 5′-ATGTGAGTGGCACCCGCTTC-3′ and antisense, 5′-ACGGTAACGACTAGGCGCTG-3′), $K_V4.3$ (sense, 5′-CCTACTACATCGGTCTGGTC-3′ and antisense, 5′-TTGCGCTTGCTGTGCAGGTA-3′), and GAPDH (sense, 5′-TGAACGGGAAGCTCACTGG-3′ and antisense, 5′-TCCACCACCCTGTTGCTGTA-3′). The PCR conditions were 5 min at 94 °C, followed by 35 cycles of 30 s at 94 °C, 30 s at 65 °C, and 30 s at 72 °C for the K_V channels, and 27 cycles of 30 s at 94 °C, 30 s at 60 °C, and 30 s at 72 °C for GAPDH. The PCR products were fractionated on 2% agarose gels and stained with ethidium bromide.

2.8. Statistical analyses

Comparisons for relative frequencies between two or three groups were tested for statistical significance using the

chi-square test or Fisher's 2-tailed exact test for 2×2 table or 2×3 table. Continuous variables were compared using Student's t-test.

3. Results

3.1. Detection of skeletal muscle-specific autoantigens by immunoprecipitation assay

Sixty-one MG sera and 30 PM/DM sera were subjected to the immunoprecipitation assay using ^{35}S-labeled RD and K562 extracts as antigen sources, and the immunoprecipitated protein profiles were compared between assays using the different extracts. Representative results obtained from MG and PM/DM sera are shown in Fig. 1A. The majority of the PM/DM sera recognized proteins shared by the RD and K562 extracts. In contrast, the MG sera precipitated only a few proteins from the RD and K562 extracts, and all the protein bands were faint. When the gels were subjected to a long film exposure (Fig. 1B), several proteins immunoprecipitated from the RD extracts, but not from the K562 extracts, showed up in some MG serum samples. These potential skeletal muscle-specific autoantigens included proteins with molecular masses of 220, 190, 70, and 60 kDa. The 70- and 60-kDa proteins were recognized by 11 (18%) of 61 MG sera, but by none of the PM/DM sera ($p=0.003$). Antibody to the 220-kDa protein was exclusively detected in 4 (6%) MG sera, but anti-190-kDa protein antibody was detected in both MG and PM/DM sera (4% and 7%, respectively). None of sera from patients with thymoma alone and healthy controls recognized any of those potential skeletal muscle-specific autoantigens. The 70- and 60-kDa proteins were always co-precipitated, although the band

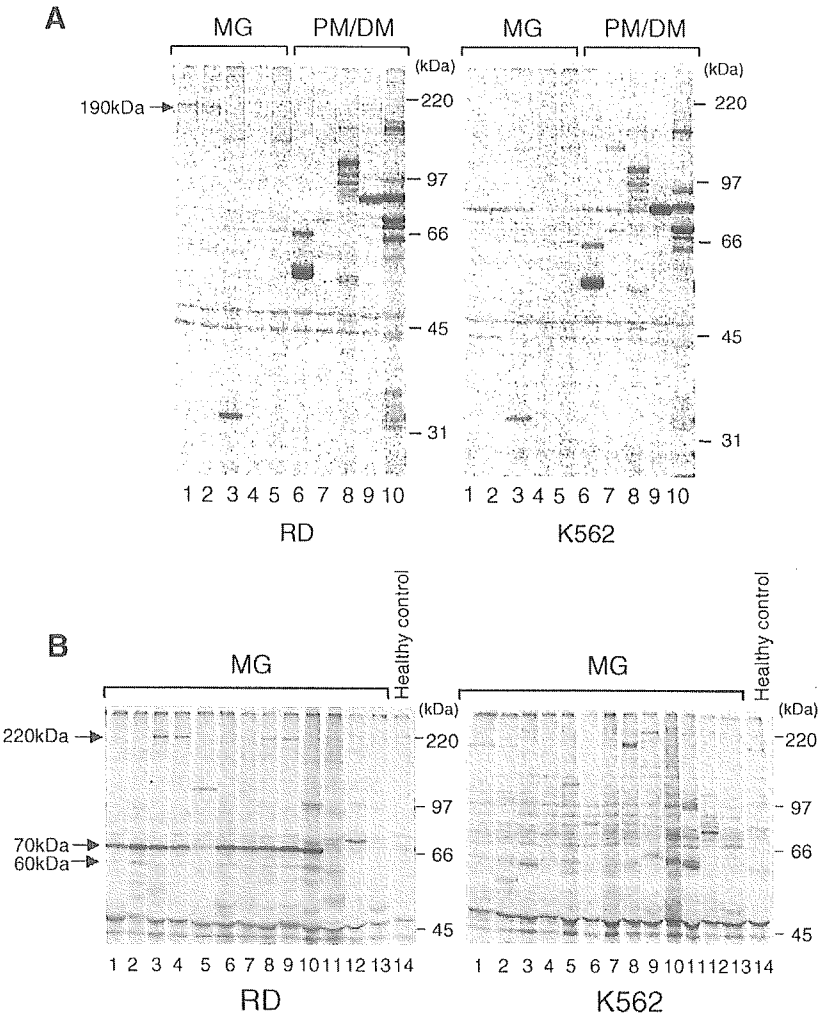

Fig. 1. Autoradiograms of immunoprecipitated ^{35}S-labeled RD and K562 extracts by sera from patients with MG. (A) Short exposure of the gels analyzing MG sera (lanes 1–5) and PM/DM sera (lanes 6–10). Immunoprecipitated materials were analyzed on SDS-8.5% polyacrylamide gels. The positions of molecular weight standards appear to the right of each panel. Arrow indicates a skeletal muscle-specific 190-kDa precipitate. (B) Long exposure of the gels analyzing MG sera (lanes 1–13) and a healthy control serum (lane 14). Arrows indicate skeletal muscle-specific 220-, 70-, and 60-kDa proteins. The 70- and 60-kDa proteins are always detected together (lanes 1–10).

intensity of the 70-kDa protein was much greater than that of the 60-kDa protein (Fig. 1B). Because the 70-kDa protein was specifically and frequently detected in the MG sera, we focused on this autoantigen in the following analysis.

3.2. Identification of the 70-kDa muscle-specific autoantigen as $K_V1.4$

The 70-kDa protein was successfully isolated from the RD extracts by affinity-purification using MG sera that contained an antibody to this protein (Fig. 2, lane 1), although contaminating immunoglobulin was present in the fraction. The 60-kDa protein was not apparent, probably because the amount isolated was too small to be detected by Coomassie blue or amino black staining. The portion of the gel corresponding to the 70-kDa protein was cut out and subjected to N-terminal amino acid sequence analysis. The amino acid sequence obtained was 5 consequent residues, *MPYGY* (shown in single-letter code). This sequence was subjected to a homology search on the NCBI database, which resulted in a complete match to only one human protein (last searched on August 25, 2004). This protein was a voltage-gated potassium channel, $K_V1.4$, which contained the MPYGY sequence at positions 17–21. A cDNA encoding human $K_V1.4$ in the database (accession number NM_002233) was isolated from skeletal muscle and has an open reading frame consisting of 653 amino acids (Philipson et al., 1990). The predicted molecular weight of $K_V1.4$ (73 kDa) was slightly larger than 70 kDa. Moreover, the N-terminal sequence of the 70-kDa protein started from position 17 of the reported $K_V1.4$ sequence. Because $K_V1.4$ is a cellular membrane protein, it might have a signal peptide at the N-terminus that is cleaved during intracellular trafficking. In fact, a potential signal peptide predicted by the Genetyx-Mac software revealed that the first 16 amino acids of $K_V1.4$ were likely to be cleaved as a signal peptide.

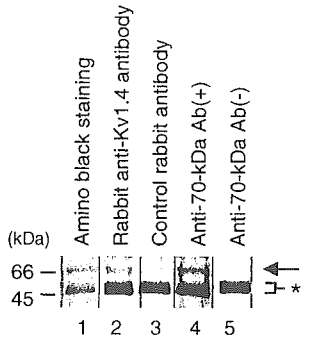

Fig. 2. Immunoblotting using an affinity-purified 70-kDa protein antigen. The affinity-purified 70-kDa was analyzed on a SDS-10% polyacrylamide gel, and stained with amino black (lane 1) or probed with rabbit polyclonal anti-rat $K_V1.4$ antibodies (lane 2), control rabbit antibodies (lane 3), MG serum with anti-70-kDa antibody (lane 4) or MG serum without anti-70-kDa antibody (lane 5). Arrow indicates a 70-kDa protein, while asterisk denotes non-specific human immunoglobulin.

A series of experiments was then carried out to test whether the 70-kDa protein targeted by the MG sera was truly $K_V1.4$. First, the affinity-purified 70-kDa protein was applied to 2-dimensional electrophoresis, revealing a PI of 4.5–5.0, which was comparable to the predicted PI of $K_V1.4$ (4.95). Second, the affinity-purified 70-kDa protein was subjected to immunoblots as an antigen source (Fig. 2). We searched for commercially available antibodies that were potentially reactive with human $K_V1.4$, and found rabbit polyclonal antibodies that had been generated by immunization with a recombinant fragment encoding the carboxyl-terminal portion of rat $K_V1.4$ (Veh et al., 1995). Since the portion of rat $K_V1.4$ used for immunization was highly homologous to human $K_V1.4$ (amino acid homology 90%), it was likely that this polyclonal antibody would recognize human $K_V1.4$ by cross-reactivity. As expected, the 70-kDa protein was recognized by the rabbit anti-rat $K_V1.4$ polyclonal antibody, but not by a control rabbit antibody (lanes 2 and 3). We further examined the reactivity to the 70-kDa protein in 4 MG sera containing the anti-70-kDa antibody, 4 sera lacking the anti-70-kDa antibody, and two healthy control sera. Of these sera, only one anti-70-kDa antibody-positive serum reacted with the affinity-purified 70-kDa protein by immunoblotting (lane 4).

Finally, cultured mouse L cells were transiently transfected with a cDNA encoding full-length human $K_V1.4$ isolated from RD. At least 10% of the cells that underwent gene transfer expressed $K_V1.4$ in the cellular membrane and cytoplasm, which was detected by the rabbit anti-rat $K_V1.4$ polyclonal antibody (Fig. 3). L cells that underwent $K_V1.4$ gene transfer were incubated with the rabbit anti-rat $K_V1.4$ antibody (red) and MG sera that contained or lacked the anti-70-kDa antibody (green). A representative serum that contained the anti-70-kDa antibody produced membranous and cytoplasmic staining on cells that overlapped with staining by the anti-rat $K_V1.4$ antibody (upper panel). Analogous findings were observed using 3 additional MG sera containing the anti-70-kDa antibody. In contrast, serum samples from 4 MG patients that lacked the anti-70-kDa antibody and 2 healthy controls did not show any staining on the $K_V1.4$-transfected cells (middle panel). Specificity of the staining was confirmed by the lack of staining on L cells transfected with a control plasmid lacking the cDNA insert (lower panel). Taken together, these findings indicate that the 70-kDa protein detected by the immunoprecipitation assay was $K_V1.4$.

3.3. Clinical features associated with the anti-$K_V1.4$ antibody in MG patients

Since results obtained from immunoprecipitation assay using RD and K562 extracts and those from immunohistochemistry on the human $K_V1.4$-expressing L cells were concordant with each other, sera immunoprecipitated the 70-kDa protein from the RD extracts, but not from the K562 extracts, were regarded as positive for anti-$K_V1.4$ antibody.

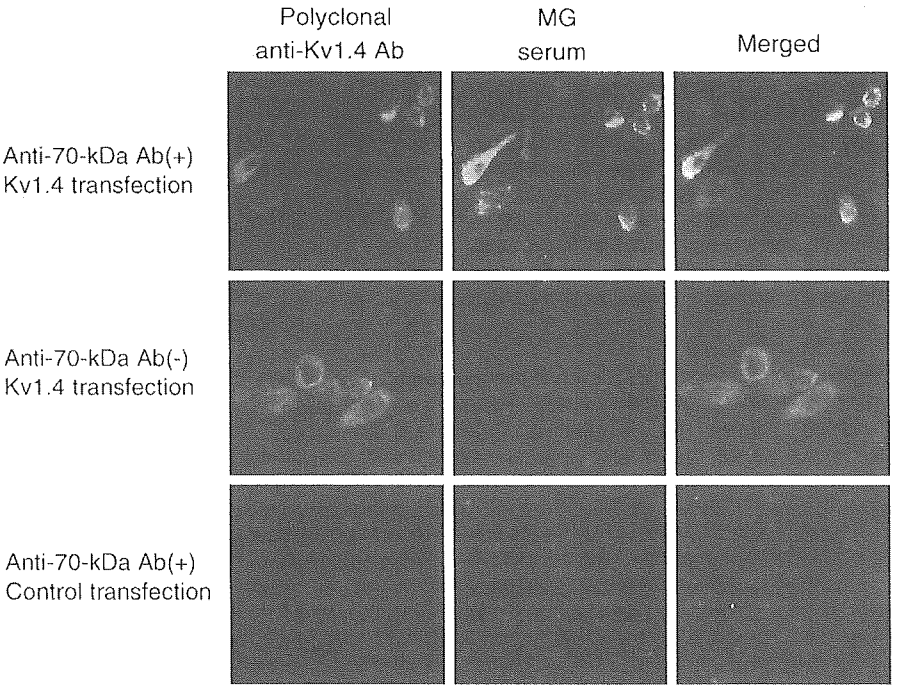

Fig. 3. Indirect immunofluorescence on mouse L cells induced to express human $K_V1.4$ by transient gene transfer. L cells transfected with a plasmid harboring human $K_V1.4$ or an empty plasmid were fixed and subjected to double-staining with rabbit polyclonal anti-rat $K_V1.4$ antibodies (red) and MG sera with anti-70-kDa antibody or without anti-70-kDa antibody (green). The cells were examined with a confocal laser fluorescent microscope. Original magnification: ×40.

Demographic and clinical findings were compared between 11 MG patients with the anti-$K_V1.4$ antibody and 50 MG patients without the antibody (Table 1). There was no difference in sex, age at MG onset, or disease duration between the two groups. All but one anti-$K_V1.4$-positive patient had generalized MG, and the frequencies of bulbar involvement and episodes of myasthenic crisis were significantly higher in patients with anti-$K_V1.4$ antibody than those without ($p<0.0001$ and $p=0.006$, respectively). In fact, the frequency of patients with severe disease, such as grade III or higher according to the Task Force of the Medical Advisory Board of the Myasthenia Gravis Foundation of America (Jaretzki et al., 2000), was greater in the anti-$K_V1.4$ antibody-positive group ($p=0.0002$). All the anti-$K_V1.4$-positive patients were seropositive for anti-AChR antibody, and there was no difference in anti-AChR antibody levels between patients with and without anti-$K_V1.4$ antibody. Thymoma diagnosed by imaging tests was more frequent in the anti-$K_V1.4$-positive than in the negative patients ($p<0.0001$). The association of anti-$K_V1.4$ antibody with thymoma was also confirmed when the subjects were restricted to 34 patients who had undergone histopathologic examination ($p=0.004$).

When the frequencies of additional diseases concomitant with MG were compared between the two groups, it was noted that myocarditis excluding viral or ischemic etiology was exclusively found in the anti-$K_V1.4$-positive group. In addition, one patient with the anti-$K_V1.4$ antibody developed acquired neuromyotonia, a disease known to be caused by autoantibodies to neuronal K_V channels (Shillito et al., 1995). Myocarditis developed after the onset of MG and thymectomy in 3 patients, who had diffuse or focal ventricular hypokinesis detected by echocardiogram. Two of these patients recovered after corticosteroid pulse therapy, although the remaining patient died of heart failure. In this case, the myocarditis did not respond to extensive immunosuppressive therapies consisting of high-dose corticosteroids, tacrolimus, and intravenous immunoglobulin. The detection of the anti-$K_V1.4$ antibody preceded the clinical onset of myocarditis in these 3 patients.

The potential relationship between the anti-$K_V1.4$ antibody and dysfunctional cardiac electrophysiology was further assessed by comparing the electrocardiographic findings between patients with and without the anti-$K_V1.4$ antibody. The frequency of QT prolongation was significantly greater in patients with the anti-$K_V1.4$ antibody than in those without ($p=0.0009$). No patients were thought to have died from lethal arrhythmia during the disease course in either the anti-$K_V1.4$-positive or negative group.

Because of the strong association between anti-$K_V1.4$ antibody and thymoma, observed clinical associations with anti-$K_V1.4$ antibody in MG patients might merely reflect the associations of these clinical features with thymoma, rather than anti-$K_V1.4$ antibody. To exclude this possibility, clinical features except thymoma were again compared within 21 MG patients with thymoma according to the presence ($n=10$) or absence ($n=11$) of anti-$K_V1.4$ antibodies. Frequencies of bulbar involvement, maximum MG severity of grade III or higher, and QT prolongation on electrocardiogram were again significantly different

($p=0.007$, 0.004, and 0.03, respectively), while differences in frequencies of myasthenic crisis and concomitant myocarditis did not reach statistical significance.

3.4. Expression of $K_V1.4$ mRNA in the abnormal thymus tissue from MG patients

The expression of $K_V1.4$ mRNA was examined in several cultured cell types and a panel of normal tissues (Fig. 4A). As expected, $K_V1.4$ mRNA was detected in RD but not K562 cells, confirming the skeletal muscle-specific nature of $K_V1.4$ that was determined by the immunoprecipitation assay. A primary culture of human myoblasts also expressed $K_V1.4$ mRNA. In normal tissues, $K_V1.4$ mRNA was detected in the skeletal muscle, heart, and brain, as reported in previous studies (Philipson et al., 1990; Tamkun et al., 1991), but not in other tissues, including the thymus. When the mRNA expression of other K_V subunits was examined in the RD cell line as well as in skeletal muscle and brain tissues, different expression profiles were observed: $K_V1.3$, 1.5, and 1.6 in RD cells; $K_V1.3$ and 1.6 in skeletal muscle; and $K_V1.3$, 1.5, 4.2, and 4.3 in brain (Fig. 4B). Since mRNA for the AChR α chain, a major target of autoantibodies in MG patients, is known to be expressed in the thymoma tissue from MG patients (Wakkach et al., 1996), abnormal thymus tissue from MG patients with and without the anti-$K_V1.4$ antibody was examined for the expression of $K_V1.4$ mRNA. $K_V1.4$ mRNA was detected in all three thymoma tissues and one of two thymic hyperplasia tissues from MG patients (Fig. 4C), but the serum from only two of the patients with thymoma was positive for the anti-$K_V1.4$ antibody.

Table 1
Demographic and clinical findings in MG patients with or without serum anti-$K_V1.4$ antibody

Demographic and clinical findings	Anti-$K_V1.4$ antibody		p
	Positive ($n=11$)	Negative ($n=50$)	
Female (number, %)	6 (54)	31 (62)	NS
Age at disease onset (years; mean ± SD)	47.0 ± 7.7	42.9 ± 19.5	NS
Disease duration (years; mean ± SD)	9.8 ± 6.9	8.5 ± 6.9	NS
Disease subset (number, %)			
Ocular MG	1 (9)	19 (38)	NS
Generalized MG	10 (91)	31 (62)	NS
Bulbar involvement (number, %)	10 (91)	10 (20)	<0.0001
Myasthenic crisis (number, %)	5 (45)	4 (8)	0.006
Maximal MG severity (number, %)[a]			
Grade III of higher	9 (81)	10 (20)	0.0002
Anti-AChR antibody (number, %)	11 (100)	43 (86)	NS
Thymoma (number, %)			
Detected by CT and/or MRI	10 (91)	11 (22)	<0.0001
Confirmed by histology[b]	10/10 (100)	11/24 (45)	0.004
Concomitant diseases (number, %)			
Autoimmune thyroid disorders[c]	1 (9)	6 (12)	NS
Myocarditis	3 (27)	0 (0)	0.004
Acquired NMT	1 (9)	0 (0)	NS
Electrocardiographic finding (number, %)			
QT prolongation	4 (36)	0/45 (0)	0.0009

CT, computed tomography; MRI, magnetic resonance image.
[a] MG severity was graded according to the Task Force of the Medical Advisory Board of the Myasthenia Gravis Foundation of America (Jaretzki et al., 2000).
[b] Histologic evaluation was done in 34 patients who received thymectomy.
[c] Gravis' disease or Hashimoto's thyroiditis.

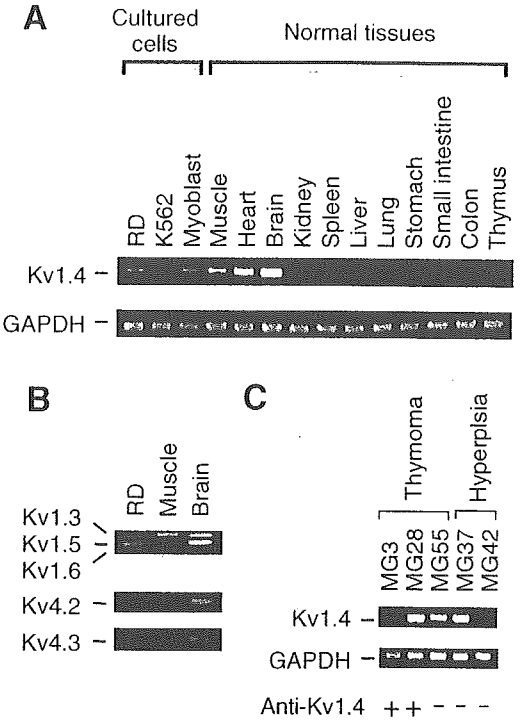

Fig. 4. mRNA expression of $K_V1.4$ and other K_V channel subunits in various cultured cells and tissues. PCR products were fractionated on 2% agarose gels and stained with ethidium bromide. (A) Expression of $K_V1.4$ mRNA in cell lines (RD, K562, and primary cultured myoblasts) and various normal tissues. The sizes for the products of $K_V1.4$ and GAPDH are 474 and 307 bp, respectively. (B) Expression of mRNAs for $K_V1.3/1.5/1.6$, $K_V4.2$, and $K_V4.3$ in RD, as well as skeletal muscle and brain tissues. PCR for $K_V1.3/1.5/1.6$ was performed using a common primer set and the sizes of $K_V1.3$, $K_V1.5$, and $K_V1.6$ are 623, 565, and 509 bp, respectively. The sizes for the products of $K_V4.2$ and $K_V4.3$ are 623 and 544 bp, respectively. (C) Expression of $K_V1.4$ mRNA in the thymus tissue obtained from 5 patients with MG in the presence or absence of anti-$K_V1.4$ antibody. Three had thymoma and two had thymic hyperplasia confirmed by histologic examination.

4. Discussion

We have identified a novel autoantibody to $K_V1.4$, one of the α subunits of the K_V channels in sera from MG patients. The identification of the 70-kDa autoantigen as $K_V1.4$ was based on the following: (i) the N-terminal amino acid sequence of the 70-kDa protein completely matched to the sequence of human $K_V1.4$; (ii) the molecular weight and PI of the 70-kDa protein were nearly concordant with the

predicted values of $K_V1.4$; (iii) polyclonal antibodies to rat $K_V1.4$ cross-reacted with the affinity-purified 70-kDa antigen; and (iv) MG sera containing the anti-70-kDa antibody and anti-rat $K_V1.4$ polyclonal antibodies exclusively stained cells that were induced to express human $K_V1.4$ by gene transfer. K_V channels consist of 4 transmembrane α-subunits that combine as homo- or hetero-tetramers (Yellen, 2002). In immunoprecipitation assays, the antigen was precipitated in the form of a protein complex. Since RD cells express several types of *Shaker*-type K_V1 family proteins other than $K_V1.4$ (Veh et al., 1995), the 60-kDa protein that was co-immunoprecipitated with $K_V1.4$ by MG sera may correspond to other K_V subunits, such as $K_V1.3$, $K_V1.5$, and $K_V1.6$. The transfection experiment indicated that the presence of $K_V1.4$ was essential to the antibody recognition, but the possibility that the autoantibody in MG sera recognizes another protein within the protein complex whose antigenicity is enhanced by binding to $K_V1.4$ cannot be entirely excluded.

Anti-$K_V1.4$ antibody was not detected in patients with PM/DM or those with thymoma alone, indicating that the anti-$K_V1.4$ antibody might be a diagnostic marker for MG, although additional studies evaluating a large series of sera from patients with various autoimmune and neurologic diseases are necessary. The anti-$K_V1.4$ antibody was clinically associated with bulbar involvement, myasthenic crisis, maximum MG severity of grade III or higher, thymoma, concomitant myocarditis, and QT prolongation on electrocardiogram, but some of these associations could be explained by the strong association between anti-$K_V1.4$ antibody and thymoma. However, the association of anti-$K_V1.4$ antibody with a severe MG subtype was also detected within MG patients with thymoma, suggesting that this antibody response is potentially useful for classifying a subset of MG patients with severe neuromuscular involvement. To confirm clinical usefulness of anti-$K_V1.4$ antibody for the disease classification in patients with MG, we have already started a prospective study involving a large cohort of MG patients, in whom antibodies to $K_V1.4$ and other K_V channels as well as antibodies to AChR, titin, and ryanodine receptor are measured at first visit.

Another interesting characteristic of the anti-$K_V1.4$ antibody was its association with myocarditis and QT prolongation on an electrocardiogram. It has been reported that cardiac diseases, such as arrhythmia, heart failure, and sudden death, are often found in MG patients, especially those with thymoma (Hofstad et al., 1984; Namba et al., 1974; Evoli et al., 2002). Since the detection of anti-$K_V1.4$ antibody preceded the clinical onset of myocarditis in all 3 patients with this complication, cardiac function should be carefully monitored in MG patients who have this antibody. In addition, the clinical association between anti-$K_V1.4$ antibody and the QT prolongation suggests that the anti-$K_V1.4$ antibody may directly affect K_V channels in the heart and induce electrophysiologic dysfunction. Since $K_V1.4$ is reported to form fast inactivating A-type channels with other subfamily components, such as $K_V4.2$ and $K_V4.3$, in the heart (Wickenden et al., 1999), impaired K_V channels containing $K_V1.4$ might lead to insufficient outward K^+ current in cardiomyocytes, resulting in prolongation of the ventricular repolarization time. Further studies examining whether anti-$K_V1.4$ antibody in patients' sera affects the function of K_V channels are necessary to clarify the pathogenic role of the antibody.

There are several features shared by the anti-$K_V1.4$ and anti-AChR autoantibody responses. First, the target antigens are cell surface channels expressed on skeletal muscles that form as multimers. Second, both antibodies in patients' sera primarily recognize a conformational epitope present on the native multimers. $K_V1.4$ was recognized by autoantibodies in patients' sera by immunoprecipitation assay and indirect immunofluorescence using cells undergoing $K_V1.4$ gene transfer, but its antigenicity was poor in immunoblots using affinity-purified $K_V1.4$. In the immunoprecipitation and indirect immunofluorescence assays, $K_V1.4$ was recognized in the form of a homo- or hetero-tetramer, while $K_V1.4$ was denatured in immunoblots. Finally, both $K_V1.4$ and the AChR α subunit were upregulated in the abnormal thymus of MG patients. Liyanage et al. showed that the mRNAs for several *Shaker*-type K_V channels ($K_V1.3$, 1.5, and 1.6) are expressed in the thymoma of MG patients (Liyanage et al., 1998). In the present study, $K_V1.4$ mRNA was expressed in both the thymoma and thymic hyperplasia tissues from MG patients, but not in normal thymus, although sources for normal and abnormal thymus were different. Since the presence of the anti-$K_V1.4$ antibody was closely associated with thymoma, an ectopic expression of $K_V1.4$ in the abnormal thymus of MG patients may be implicated in the initiation of the autoimmune response to $K_V1.4$, as reported for the anti-AChR antibody response (Wakkach et al., 1996).

Autoantibodies to neuronal K_V channels are also known to contribute to the pathogenesis of acquired neuromyotonia, characterized by the hyperexcitability of motor nerves, leading to muscle twitching, cramps, and weakness (Newsom-Davis and Mills, 1993; Shillito et al., 1995). Autoantibodies in patients with acquired neuromyotonia recognize several different subunits of neuronal K_V channels, which are structurally related to the "*Shaker*-related" K_V1 family (Hart et al., 1997). In our study, one of the MG patients with anti-$K_V1.4$ antibody had concomitant neuromyotonia. Taken together with the finding that MG patients with thymoma sometimes develop acquired neuromyotonia (Newsom-Davis and Mills, 1993; Shillito et al., 1995; Evoli et al., 2002), those patients might be prone to develop an autoimmune response to both muscular and neuronal K_V channels.

Acknowledgements

This work was supported by grants from the Japanese Ministry of Education, Science, Sports and Culture (to S.S.,